[redacted]

JET PROPULSION LABORATORY
CALIFORNIA INSTITUTE OF TECHNOLOGY
PASADENA 3, CALIFORNIA

National Aeronautics and Space Administration

(NASA Contract No. NASw-6)

(NASA CR-51076; JPL-TR-34-59)

Technical Release No. 34-59

EXPERIMENTAL INVESTIGATION OF EXHAUST DIFFUSERS FOR ROCKET ENGINES

Paul F. Massier and
E. John Roschke

May 5, 1960

(2) mp

22 pp

Copy No._____

JET PROPULSION LABORATORY
A Research Facility of
National Aeronautics and Space Administration
Operated by
California Institute of Technology
Pasadena, California
May 5, 1960

CONTENTS

Introduction 1

General Discussion of Rocket-Engine Exhaust Diffusers 3

Experimental Program 6

Experimental Apparatus 7

1. Nozzles 7

2. Diffuser Parts 8

3. Instrumentation 10

4. Test Procedure 12

Experimental Results 13

1. Constant-Area-Duct Type Diffusers 16

2. Second-Throat Type Diffusers 17

3. Additional Observations on Second-Throat Type Diffusers 20

a. Diffuser cavity diameter 20

b. Diffuser entrance section 21

c. Subsonic cone angle and area ratio 22

d. Time interval 22

e. Heat transfer 23

f. Conical nozzles 24

4. Auxiliary Methods of Starting and Operating Second-Throat Type Diffusers 24

a. Experiments conducted with a diffuser exhausting into a vacuum tank as a starting technique 24

CONTENTS (Cont'd)

b. Experiments conducted using annular ejection of a secondary gas at the exit of the subsonic diffuser 27

c. Experiments conducted using primary-gas extraction near the entrance of the second throat 29

5. The Performance of a Canted Diffuser to Simulate Nozzle Gimballing 31

The Full-Scale Diffuser 32

Conclusions 35

Nomenclature 39

Tables 41

Figures 47

Appendix A. Starting and Operating an Exhaust Diffuser Downstream of a Supersonic Nozzle 66

Appendix B. Methods of Calculating Diffuser Efficiency 70

References and Bibliography 75

TABLES

1. Gas properties and flow parameters used in experiments 41

2. Average experimental performance of various model exhaust diffusers, without auxiliary equipment 42

3. Average experimental performance of various model exhaust diffusers, with auxiliary equipment 43

4. Results obtained with constant-area-duct type diffusers with $\overline{\gamma} \sim 1.3$ and contour nozzle with $\epsilon = 20.3$ 44

5. Best results obtained with a vacuum-tank start using configuration 2 with $\overline{\gamma} \sim 1.3$, contour nozzle, $\epsilon = 20.3$ 44

6. Performance results obtained with mass extraction on start, configuration 3A, $\overline{\gamma}$ 1.22 45

7. Best results obtained with the full-scale exhaust diffuser 46

B-1. Estimated flow properties at the diffuser exit, one-dimensional calculations based on the measured weight rate of flow 74

FIGURES

1. Methods of adapting exhaust diffusers to rocket engines 47
2. Experimental diffuser configurations 48
3. Theoretical nozzle-diffuser performance based on one-dimensional, normal-shock flow theory. 49
4. Efficiency of a normal shock located at the nozzle exit 50
5. External view of a typical model exhaust diffuser of second-throat type, showing method of spray cooling 50
6. Diffuser area ratio as a function of distance from nozzle exit 51
7. Average experimental values for minimum starting and operating system pressure ratios; for model exhaust diffusers used with a contour nozzle, $\epsilon = 20.3$ 52
8. Calculated efficiencies for model exhaust diffusers used with a contour nozzle, $\epsilon = 20.3$ 52
9. Typical exhaust-diffuser performance, constant-area-duct type diffuser 53
10. Typical static-pressure distribution at the wall, constant-area-duct type diffuser 53
11. Typical exhaust-diffuser performance, second-throat type diffuser, configuration 2, $\overline{\gamma} \sim 1.3$ 54
12. Typical exhaust-diffuser performance, second-throat type diffuser, configuration 2, $\overline{\gamma} \sim 1.22$ 54

FIGURES (Cont'd)

13. Typical exhaust-diffuser performance, second-throat type diffuser, configuration 3, $\bar{\gamma}\sim1.22$ 55
14. Typical exhaust-diffuser performance, second-throat type diffuser, configuration 3, $\bar{\gamma}\sim1.3$ 56
15. Typical exhaust-diffuser performance, second-throat type diffuser, configuration 3, $\gamma = 1.4$ 57
16. Effect of second-throat length on the performance of configuration 2 with a fixed diffuser contraction ratio of 1.545 58
17. Typical static-pressure distribution at the wall, second-throat type diffuser, configuration 2, $\bar{\gamma}\sim1.22$ 58
18. Typical static-pressure distribution at the wall, second-throat type diffuser, configuration 3, $\bar{\gamma}\sim1.22$ 59
19. Typical static-pressure distribution at the wall, second-throat type diffuser, configuration 3, $\bar{\gamma}\sim1.3$ 59
20. Typical static-pressure distribution at the wall, second-throat type diffuser, configuration 3, $\gamma = 1.4$ 60
21. Schematic arrangement of vacuum tank apparatus 60
22. Schematic arrangement of configuration 2 modified for annular ejection of a secondary gas at the exit of the subsonic diffuser 61
23. Effect of nitrogen ejection at the diffuser exit on the operating performance of configuration 2 61
24. Configuration and apparatus for primary-gas extraction on start. . . 62

FIGURES (Cont'd)

25. Simulation of nozzle gimballing by insertion of a wedge between nozzle and diffuser inlet section 62

26. Effect of angular misalignment between diffuser and nozzle axes on diffuser performance 63

27. An exhaust diffuser designed for use with a 6000-lb-thrust rocket engine having a nozzle-expansion-area ratio of 20.0 64

28. View of exit end of full-scale exhaust diffuser 65

EXPERIMENTAL INVESTIGATION OF EXHAUST DIFFUSERS FOR ROCKET ENGINES[1]

Paul F. Massier[2]
E. John Roschke[3]

ABSTRACT

An experimental investigation was conducted of numerous configurations of supersonic exhaust diffusers. Exhaust diffusers are utilized to lower the back pressure on rocket engines, thereby allowing gas to flow through an engine nozzle without separation. Second-throat type diffusers exhibited good performance; however, the best performance was obtained when auxiliary means such as injection or extraction of mass flow were used in conjunction with second-throat type diffusers. Both contour and conical nozzles were tested and gases having specific heat ratios of 1.22, 1.3, and 1.4 were used. Full-scale diffuser performance was superior to performance obtained on tenth-scale model tests.

---

[1]This paper presents the results of one phase of research carried out at the Jet Propulsion Laboratory, California Institute of Technology, under Contract No. NASw-6, sponsored by the National Aeronautics and Space Administration.

[2]Research Group Supervisor, Heat Transfer and Fluid Dynamics Group.

[3]Senior Research Engineer, Heat Transfer and Fluid Dynamics Group.

SUMMARY

Rocket engines that are designed for use in the Earth's upper atmosphere or in space require a low pressure environment when tested at ground level in order to evaluate the performance of all system components. Performance information such as thrust and thrust-chamber heat transfer can be obtained under certain conditions with the use of exhaust diffusers. The primary purpose of an exhaust diffuser is to reduce nozzle back pressure sufficiently to allow the nozzle to flow full at design chamber pressure, that is, without flow separation occurring in the divergent portion of the nozzle.

An extensive experimental investigation has been made of numerous axisymmetric exhaust diffuser configurations and auxiliary techniques for improving diffuser performance. Some of these experiments include the evaluation of straight constant-area tubes, second-throat type diffusers, second-throat diffusers with mass bleed upstream of the second throat during start, and second-throat diffusers with secondary mass injection. The effects on performance of geometrical variations such as length, diameter, and contraction and expansion cone angles were investigated. The effect of diffuser performance on angular misalignment between diffuser axis and nozzle axis was determined to establish the feasibility of gimballing an engine that is tested in a vacuum-chamber exhaust-diffuser facility. Tests were made using both conical and contour type convergent-divergent nozzles. Experiments were also conducted on the effects of size by using a diametrical scale factor of 10. Results were obtained with several different gases; their nominal specific heat ratios were

1.22, 1.3 and 1.4. These gases included nitrogen, the decomposition products of hydrazine, and the combustion products of nitrogen tetroxide and hydrazine.

Based on model tests for which the supersonic nozzle had a throat diameter of 0.552 in. and an expansion area ratio of 20.3:1, it was found that:

1. Second-throat type diffusers perform considerably better than the constant-area-duct type.
2. Second-throat type diffusers give the best performance when the length of the second throat is larger than 8 diameters.
3. The inlet geometry to second-throat type diffusers has a considerable effect on performance.
4. For gases having a specific heat ratio of 1.22, the minimum second-throat diameter for starting the diffuser was 7.6 per cent larger than the predicted value. For gases having specific heat ratios of 1.3 and 1.4, the variation of second-throat diameter from the predicted value was less than this.
5. Second-throat type diffusers can be successfully cooled externally with water sprays; however, areas of high local heat flux can occur under certain operating conditions.
6. Diffusers used with contour nozzles exhibit somewhat better performance than diffusers used with conical nozzles.
7. Hysteresis between starting and operating conditions in second-throat type diffusers can be virtually eliminated in some cases.
8. An angular misalignment between the nozzle axis and the second-throat diffuser axis of up to 7 deg has a slightly adverse effect on

starting chamber pressure, but lowers the operating chamber pressure by a small amount.

9. Performance of second-throat type diffusers can be improved by utilizing auxiliary means such as secondary mass injection, primary mass bleed during start, or the discharge of diffuser exhaust gases into a vacuum tank.

A substantial difference in starting and operating chamber pressure may exist between full-scale and model versions of a second-throat type diffuser. Considerably better performance was obtained with a full-scale diffuser than with the particular model design on which it was based.

INTRODUCTION

Rocket engines designed for high-altitude operation, such as those incorporated in the upper stages of a space vehicle, generally cannot be properly evaluated at design chamber pressure and ground-level ambient pressure because the gas flow will separate from the divergent portion of the nozzle wall. Performance information such as thrust, thrust-chamber heat transfer, vacuum ignition, thrust-chamber vibrational characteristics, and endurance capabilities of engine components, all under conditions of a full-flowing nozzle, is necessary to determine the operational capabilities of an engine. Therefore, to experimentally evaluate the high-altitude performance of an engine at ground level, it becomes necessary to provide some means of reducing the nozzle back pressure for time intervals specified by the engine operating requirements.

Methods of reducing the nozzle back pressure sufficiently to prevent flow separation in the nozzle include the use of altitude chambers, vacuum pumps, ejectors, and exhaust diffusers. These may be used individually or in various combinations. Altitude facilities that utilize vacuum pumps or other types of gas exhausters and have sufficient capacity to accommodate full-scale engine testing are large and expensive. Ejectors using secondary gas flow may require auxiliary mass flow rates greatly exceeding the primary mass flow rate. Exhaust diffusers utilize the momentum of the engine exhaust gases to reduce the nozzle back pressure. They are relatively simple in design and inexpensive to fabricate. The work that is covered in this investigation includes results obtained from the use of various configurations of exhaust diffusers.

A rocket-engine exhaust diffuser in its simplest form would consist of a straight, constant-diameter duct either attached directly to the engine exit or to a chamber surrounding the engine. More refined diffusers would incorporate a duct of varying area having a region of minimum cross-sectional area called a second throat (the first throat being located in the engine nozzle). Pressure recovery in the diffuser is accomplished by means of a progressive shock-wave system and gradual, but not necessarily smooth, gas deceleration to subsonic velocities. The main disadvantage of exhaust diffusers is that they have poor adaptability to engines of different size.

Research on model exhaust diffusers was applied to the design of an exhaust diffuser for a 6000-lb-thrust rocket engine. This engine has a design chamber pressure of 150 psia and a nozzle-expansion-area ratio of 20:1. The divergent portion of the thrust chamber is a shortened version of a contour nozzle originally designed for a nozzle-expansion-area ratio of approximately 55:1 by the method of characteristics. Propellants for the engine are hydrazine and nitrogen tetroxide.

An experimental program was undertaken to determine an exhaust diffuser configuration which would allow the previously mentioned nozzle to flow full at design chamber pressure and ground-level ambient pressure. Experiments were conducted using a nominal tenth-scale model of this nozzle. The throat diameter of the model nozzle was 0.552 in. Tests were made on many diffuser configurations using gases of three different specific heats. A full-scale exhaust

diffuser was subsequently designed, fabricated, and tested with a 6000-lb-thrust experimental rocket engine.

GENERAL DISCUSSION OF ROCKET-ENGINE EXHAUST-DIFFUSER OPERATION

A rocket-engine exhaust diffuser may be regarded as being an axisymmetric duct placed adjacent to the nozzle exit plane with its longitudinal axis coincident with the nozzle axis. Figure 1 illustrates two possible methods of adapting an exhaust diffuser to a rocket engine. The momentum of the engine exhaust gases is utilized to lower the nozzle back pressure to allow the nozzle to flow full. The nozzle back pressure, however, is lowered sufficiently to permit full flow only within certain engine operating regions. Figure 2 shows several diffuser configurations which have been found to be practical for rocket-engine testing. There are other configurations which may give superior performance characteristics but which appear to be impractical. Examples of the latter would include variable-geometry diffusers and other types utilizing a movable center body located internally within the diffuser near the nozzle exit plane.

Supersonic diffusers of the second-throat type generally have an operating inlet total pressure which is lower than that required for starting. Discussions of the theoretical starting procedure for a supersonic diffuser may be found in Appendix A and in textbooks on supersonic aerodynamics, for example, (1). The inlet total pressure necessary to start supersonic diffusers can be estimated by considering a normal shock wave to be located at the nozzle exit of a rocket engine and calculating the upstream total pressure assuming ambient static pressure

downstream of the normal shock. In the case of the constant-area-duct type diffuser the minimum starting total pressure is nearly the same as the minimum operating pressure. For the second-throat type diffuser, a lower operating total pressure can be achieved and can be approximately estimated by considering a normal shock wave to be located at the minimum or second-throat area and calculating the total pressure upstream of the shock assuming ambient static pressure downstream. The maximum diffuser contraction ratio (defined in this case as the nozzle exit area divided by the diffuser second-throat area) can be estimated in a similar manner.

Calculations of the type just described are performed in Appendix A, and the results of these calculations are plotted in Fig. 3. Note that in Fig. 3 the ratio of nozzle-inlet total pressure (which is also equal to the diffuser-inlet total pressure for isentropic expansion in the nozzle) to ambient static pressure has been plotted as a function of nozzle-expansion-area ratio. These parameters have been selected because they are more useful for rocket-engine work than the more frequently used parameters of total-to-total pressure ratio across the diffuser and inlet Mach number to the diffuser. Rocket-engine exhaust diffusers most generally exhaust to atmospheric pressure and the exit total pressure is difficult, if not impossible, to measure. In this case the kinetic energy of the gases at the diffuser exit is lost and further pressure recovery is not possible. If the velocity of the gases at the diffuser exit is zero, then the limiting value of the exit total pressure is atmospheric pressure. Ideally this would require a subsonic diffuser having an infinite area ratio. In the analysis presented in Appendix A, the total-to-static pressure ratio across the normal shock has been utilized rather than the total-to-total pressure ratio across the normal shock.

The results of Fig. 3 can be used to estimate the potential ability of an exhaust diffuser to accomplish its purpose. The curves labeled "minimum start" may be used for both constant-diameter and second-throat types of diffusers if the diffuser inlet area and the nozzle exit area are identical. The curves labeled "minimum operate" apply only to second-throat type diffusers. No information concerning configuration, other than maximum contraction ratio, is given by this analysis. In order to determine an optimum diffuser configuration for use with a particular engine, it is necessary to perform experiments.

Considerable research effort (2, 3, 4) has been applied toward reducing the starting and operating inlet total pressures of supersonic diffusers. However, most of the available information in the literature pertains to wind-tunnel diffusers which are part of complete wind-tunnel systems. It would be of decided advantage if diffuser performance could be accurately predicted in advance and, perhaps more important, if a diffuser configuration could be predicted which would give optimum performance. Unfortunately neither of these problems has been solved analytically because internal flow in supersonic diffusers is not yet well understood and is not amenable to rigorous analytical treatment. The design of rocket-engine exhaust diffusers is further complicated by certain engine requirements such as maximum permissible chamber pressure, instrumentation requirements, and explosion hazards. In addition, the physical dimensions of an exhaust diffuser must be considered, because existing engine test facilities may be limited in available working area, precluding the installation of a bulky exhaust diffuser.

The starting and operating nozzle pressure ratios are the most meaningful criteria for comparing the performance of different rocket-engine diffuser configurations. The diffuser efficiency alone is not absolutely indicative of over-all system performance. The reasons for this are discussed in Experimental Results. The efficiency of a supersonic diffuser can be estimated by calculating the efficiency of a normal shock wave located at the nozzle exit; these calculations are presented in Appendix B. The efficiency of a normal shock located at the nozzle exit is plotted in Fig. 4.

EXPERIMENTAL PROGRAM

The experimental program was conducted in four phases. During Phase 1, tests were made on numerous diffuser configurations using relatively cool nozzle exhaust gases, which were the decomposition products of hydrazine, and rather crude uncooled diffuser parts. The model 20.3:1-expansion-area-ratio contour nozzle is described in the section entitled Nozzles. The purpose of Phase 1 was to determine the general type of diffuser configuration which would give the best performance results when used with the nozzle specified.

During Phase 2, some of the more promising configurations were tested using both nitrogen gas and the products of combustion of hydrazine and nitrogen tetroxide. It was necessary to use a cooled combustion chamber, nozzle, and diffuser parts for these bipropellant tests. The diffuser parts used during Phase 2 were more carefully fabricated and fitted than the parts used during Phase 1. The inner contours were smoother, axial gaps were eliminated between parts, and matching of internal diameters between successive parts was more

accurately controlled. It was during Phase 2 that the design of the full-scale exhaust diffuser was completed and fabrication initiated based on the model diffuser configuration which had given the best performance during Phase 1.

During Phase 3, attempts were made to improve the starting and operating characteristics of certain model diffuser configurations by auxiliary means. Tests were made using two primary gases, the decomposition products of hydrazine, and the products of combustion of hydrazine and nitrogen tetroxide. During these tests a diffuser configuration was discovered which had considerably better starting characteristics, without the aid of any auxiliary equipment, than the best configuration determined previously. This new configuration was then extensively tested using all three primary gases previously mentioned. By this time fabrication of the full-scale diffuser was in an advanced stage, so that the design of the full-scale diffuser was not immediately altered.

During Phase 4, several additional configurations were tested using the bipropellant products of combustion. Also, certain miscellaneous tests were made to determine the effect of angular misalignment between nozzle and diffuser axes,as well as diffuser cooling techniques. The full-scale diffuser was put into successful operation before the termination of Phase 4.

EXPERIMENTAL APPARATUS

1. Nozzles

In all cases, nozzles used for the model tests had a throat diameter of 0.552 in. and an expansion area ratio of 20.3. Variations in dimensions between different nozzles were less than 0.5 per cent. The divergent portion of the

contour nozzle was designed for $\gamma = 1.22$ by the method of characteristics, and had an initial divergence half-angle of 22° 55' and an exit divergence half-angle of 12° 50'. Limited tests were made with a conical nozzle having a divergence half-angle of 17° 50'. The length of the conical nozzle from the throat to the exit plane was approximately the same as the equivalent dimension of the contour nozzle.

Nozzles used in the bipropellant tests (the combustion products of N_2O_4 and N_2H_4) were fabricated from nickel-plated mild steel or nickel-plated copper and had a nominal wall thickness of 0.050 to 0.070 in. These nozzles were cooled by water circulated tangentially through a concentric cooling jacket. Because of the manner in which the nozzle was installed in the cooling jacket, it became necessary to provide film cooling for the converging portion of the nozzle, primarily for the protection of a rubber O-ring seal. The nozzles were provided with one 0.020- to 0.030-in.-diameter static-pressure tap with the hole centerline located 0.035 in. from the nozzle exit plane at an area ratio of 20:1.

Nozzles used in the monopropellant tests were fabricated from 347 stainless steel. These nozzles were not cooled except by radiation and natural convection. Eleven pressure taps were located in the nozzles between throat and exit. Pressure taps were located spirally around the periphery of each nozzle and were drilled normal to the inner contour of the nozzle. These same nozzles were also used in the tests for which the working fluid was nitrogen gas.

2. Diffuser Parts

Various diffuser configurations were assembled from individual flanged sections. In the case of constant-area-duct type diffusers, the configuration consisted of only one section. In the case of second-throat type diffusers,

however, the configuration consisted of as many as five sections, depending on the particular configuration. All diffuser configurations and individual sections were used interchangeably for all three primary gases, the only difference being in the manner of cooling. Diffuser configurations used in the monopropellant or nitrogen gas tests were not cooled except by radiation and natural convection; those used in the bipropellant tests were cooled by water sprays impinging on the exterior surfaces of the diffuser.

Diffuser parts used in the early stages of the program, e.g., during Phase 1, were crudely fabricated to facilitate a rapid testing schedule. Individual sections were made of mild steel, in many cases Shelby tubing, with serrated flanges welded to both ends. To assemble a configuration for testing, parts were merely bolted together with ring-shaped copper gaskets inserted between individual parts.

Alignment of parts was accomplished by visual observation and manual radial adjustment of flanges. Because of the gaskets, axial gaps approximately 0.030 in. in width existed between parts. No special attention was given to the surface finish of interior surfaces.

A new method of fabricating diffuser parts was initiated during Phase 2: flanges were fabricated with locating rings and slots at either end of a part, respectively, and an attempt was made to secure better finishes on interior surfaces. Such parts could be assembled quickly with greater alignment accuracy, and the axial gaps between parts were virtually eliminated. These parts were also made of mild steel. Figure 5 shows a photograph of a typical second-throat type diffuser with parts fabricated by the second method described

above. This particular diffuser consisted of three individual sections bolted together. The method of spray cooling employed is clearly evident in the photograph. Note the pressure taps located at regular intervals along the top of the diffuser. These pressure taps were connected to a bank of mercury manometers by long copper tubes. The model exhaust diffuser in Fig. 5 is bolted directly to the nozzle coolant jacket in preparation for a bipropellant test.

3. Instrumentation

In all tests the static pressure at the wall was measured in the constant-area combustion chamber immediately preceding the nozzle by means of a 0-600 psig Statham pressure transducer. The nozzle-inlet total pressure was obtained from these readings by the usual one-dimensional Mach number correction. It is estimated that the accuracy of measurement of the nozzle-inlet total pressure was well within the ±1 per cent of full scale, or ±6 psi, of the pressure transducer's listed accuracy.

When liquid propellants were used, the primary mass flow rate was measured prior to decomposition or combustion by orifice plates and Foxboro differential pressure transducers located in the liquid supply lines. The mass flow rate of nitrogen gas was measured by means of a calibrated venturi located upstream of the primary nozzle.

Barometric pressure was measured at the test site prior to all experimental tests by means of a commercial mercury barometer. Static wall pressures in the nozzle and exhaust diffuser were measured by mercury manometers. Each static-pressure tap was connected to a common-well type manometer bank by

means of long lengths of 1/8-in. copper tubing (see Fig. 5). Lengths of this tubing varied between 10 and 15 ft. The entire manometer bank was photographed at desired test points by a Speed Graphic 4x5-in. camera. It is estimated that the accuracy of measurement of wall static pressures in the nozzle and the diffuser was within ±0.10 in. of mercury, or approximately ±0.05 psi. Factors which enter into this accuracy include (1) reading accuracy of barometric pressure, (2) inclusion of dirt and contaminants in the mercury, (3) possibility of minute leaks in the system, (4) variations in mercury-column heights due to slight departures from steady-state pressures, (5) parallax error due to camera placement, and (6) reading errors in the mercury-column heights from the photographs. The cavity pressure p_{b} in addition to being measured by a mercury column, was also recorded during experimental tests by means of a 0-30 psia Statham pressure transducer. This reading, however, was used only as an instantaneous indication of whether or not the diffuser had started and was not used as an absolute measurement in the data reduction.

Nozzle-inlet gas temperature was measured by means of a platinum--platinum-10 per cent rhodium shielded thermocouple during the monopropellant tests and by means of a chromel-alumel thermocouple during the nitrogen gas tests. Gas temperatures were not measured in the bipropellant tests.

All parameters depending on electrical means of measurement, such as pressure transducers and thermocouples, were recorded on pen-type Speedomax recorders. No thrust measurements were made during any of the tests.

4. Test Procedure

All pressure transducers were periodically calibrated to insure that the instruments were not damaged and that there were no radical departures from earlier calibrations. The manometer tubes and the mercury were occasionally cleaned to insure that photographs of readable quality were obtained. All diffuser configurations were systematically and periodically checked for leaks by both excess-pressure and vacuum tests on the entire system. The partial or total blockage of pressure taps and manometer leads was somewhat of a problem on the monopropellant tests and became an aggravating problem on the bipropellant tests. For this reason great care was taken to insure that at least the nozzle exit and the cavity pressure lines were clear of blockage before conducting a test. During bipropellant tests such checks became necessary before each individual test.

The minimum starting total pressure at the nozzle inlet was determined in two ways: (1) by steadily increasing the total pressure and noting at what value the nozzle began to flow full by observation of the nozzle exit pressure; (2) by making individual tests starting at successively lower values of total pressure and noting at what limiting value the nozzle would not flow full--even if allowed to run for a considerable length of time--again by observing the nozzle exit pressure. Procedure (2) is recommended because this method is not highly dependent on the response time of the manometer pressure lines. A definite change in the tonal quality of the noise emitted by the diffuser exhaust jet was found to occur when the diffuser started and the nozzle began to flow full; but this

tonal change is not recommended as a good criterion for judging precisely when the nozzle begins to, or ceases to, flow full.

The minimum operating total pressure was determined by starting the diffuser at a high total pressure so that the nozzle was definitely flowing full, and then reducing total pressure, which is the reverse procedure to that outlined in method (1) above.

All test points and all photographs of the manometer bank were obtained under conditions of steady-state operation.

EXPERIMENTAL RESULTS

Many experimental diffuser configurations have been tested, but space would not permit a detailed account of the performance data of all of these. The performance data of three diffuser configurations as shown in Fig. 2 are included. Configuration 1 is a constant-area-duct type diffuser, and configurations 2 and 3 are second-throat type diffusers. Configuration 2 was selected for discussion because it was used as the basis of design for the full-scale diffuser. Configuration 3 produced the best performance for gas flow consisting of the products of combustion of N_2O_4—N_2H_4 when no auxiliary starting or operating equipment was used in conjunction with the diffuser. Figure 6 shows the variation of diffuser cross-sectional area ratio A/A_e with axial length for configurations 2 and 3.

In Table 1 a summary of estimated gas properties and flow parameters is given for the three gases that were used. Tables 2 and 3 present a summary of performance parameters for several model exhaust-diffuser configurations with and without auxiliary equipment. Some of this data is plotted in Figs. 7 and 8 using

γ as the independent variable. In Table 2 there appear to be relatively large discrepancies in the measured values of p_e/p_t for different configurations when using the same gas and the same type of nozzle (contour or conical). These discrepancies could have been caused by many factors, which include (1) measurement errors as discussed in Instrumentation, Experimental Apparatus, (2) changes in total temperature and gas composition during monopropellant tests with consequent changes in the molecular weight of the gases, (3) changes in total temperature and gas composition during bipropellant tests due to varying mixture ratio, (4) the effect of introducing water for film-cooling the combustion chamber and converging portion of nozzles used in bipropellant tests, (5) surface roughness due to erosion and pitting of the nickel plating on the interior surface of nozzles used in the bipropellant tests (an effect which increased with the number of tests conducted on a given nozzle), and (6) possible effects of the magnitude of p_b on the magnitude of p_e by boundary-layer feedback. It is not known to what extent these factors affected the thrust since no thrust measurements were made.

In Fig. 7 the system pressure ratios for starting and operating are shown by the solid curves as predicted by the normal-shock theory developed in Appendix A. If just those diffusers are considered that did not employ auxiliary equipment, only configuration 3 exhibited a starting point less than predicted by theory for $\overline{\gamma} \sim 1.22$ or $\overline{\gamma} \sim 1.3$. For nitrogen, which has a γ of 1.4, none of the configurations had an operating point as low as that predicted by theory, with the exception of configuration 3. Note that for $\gamma = 1.4$ both the starting point and the operating point for configuration 3 are in accordance with the normal-shock prediction. Figure 7 shows that a complete description of diffuser performance cannot be

obtained by using γ as a correlation parameter for gases differing significantly in physical properties.

The diffuser efficiency calculation by the method indicated in Appendix B is shown for various configurations in Fig. 8. It was stated previously that system pressure ratio is a more meaningful criterion for judging the performance of rocket-engine diffusers than the diffuser efficiency. This statement requires explanation. For one-dimensional flow it is possible to develop an analytical relationship between the static pressures at the entrance and exit of a supersonic diffuser, the entrance total pressure, γ, and the diffuser efficiency. In order to transform this relationship into one which utilizes the inlet total pressure to a nozzle placed upstream of this diffuser, it is necessary to make some assumptions regarding both nozzle losses and the relationship between the static pressure at the nozzle exit and the static pressure at the diffuser entrance. It is assumed that the total pressure at the nozzle entrance and the diffuser entrance are equal and that the relationship between actual values p_e and p_b is disregarded. The consequences of these assumptions are demonstrated by the results shown in Fig. 8. Not shown in Fig. 8 is the efficiency of a normal shock located at the throat of a second-throat type diffuser using the maximum possible contraction ratio; this curve would have been situated above the one shown by only 2 to 3 per cent as measured on the ordinate scale. The points shown in Fig. 8 do not bear the same relationship to the theory as the corresponding points of Fig. 7, a result caused by the unpredictable relationships that exist between p_e and p_b as demonstrated in Table 2, and by the fact that diffuser efficiency η_d utilizes p_b instead of p_e.

Published experimental data on the performance of exhaust diffusers designed for use with rocket engines, particularly data obtained using hot gases, is not plentiful. References (5) and (6) contain some useful data on rocket-engine exhaust diffusers; however, most of these data were obtained using cold gases.

1. Constant-Area-Duct Type Diffusers

The decomposition products of hydrazine were used for all tests on the constant-area-duct type diffuser. The cavity pressure p_b was not measured since the first pressure tap in the diffuser was located at $x/D = 0.2$ from the nozzle exit plane. Typical performance data for a constant-area-duct type diffuser are shown in Figs. 9 and 10.

Figure 9 shows the variation of the nozzle-exit pressure ratio p_e/p_a with the nozzle-inlet total pressure ratio p_t/p_a, and the regions where the nozzle flow was separated, as well as regions where the nozzle was flowing full. Results for this type of diffuser using various D/D_e and L/D are shown in Table 4. Discrepancies between measured values of p_e/p_a for the two cases of D/D_e listed are apparent when the corresponding values of p_t/p_a are considered; possible reasons for this have been discussed previously. In general, constant-area-duct type diffusers exhibit no measurable hysteresis; that is, the minimum starting total pressure is equal to the minimum operating total pressure.

Figure 10 shows typical pressure distributions measured along the wall of the diffuser. The difference in the pressure distributions between a nozzle with separated flow and a nozzle with non-separated flow is substantial. At pressure ratios above starting, the axial position at which sharply increasing static pressure occurs increases as the nozzle-inlet total pressure is increased.

A theoretical model of one-dimensional flow in this type of diffuser is discussed in references (5) and (7). If $p_b = 0$, and $D = D_e$, this theory yields values of the minimum system pressure ratio for starting that are identical to the results of the normal-shock theory given by the solid curves of Fig. 3. For ducts having $D \neq D_e$ these results can be corrected by a multiplication factor of A/A_e. Computations of $(p_t/p_a)_{min}$ and $(p_e/p_a)_{min}$ which appear in Table 4 were computed by the methods just outlined. Note that the computed values of the performance parameters listed underestimate the measured values by rather large amounts.

2. Second-Throat Type Diffusers

The performance data of configurations 2 and 3 are plotted in Figs. 11 - 12 and 13 - 15. Although the general trends of all these performance curves are similar, there are significant differences in the magnitudes of p_e/p_a, p_b/p_a, the amount of hysteresis, and the minimum starting and operating regions. These differences exist in comparisons of configurations and comparisons of different gases using the same configuration. In general, as p_t/p_a is increased from some low value for which flow separation occurs in the nozzle, a point is reached when the nozzle suddenly flows full and the diffuser starts. This is the minimum starting point of the diffuser. The system pressure ratio can then be reduced until at some minimum value the nozzle will suddenly cease to flow full and the separation point returns to the nozzle. The cross-hatched regions shown in Figs. 11 - 15 are judged to be the minimum starting and operating regions of the particular cases. A wider range of system-pressure-ratio values for the minimum starting region exists for configuration 2 than for configuration 3.

Experiments made on configuration 2 established $\psi = 1.545$ as the maximum contraction area ratio for which the diffuser would start using either the monopropellant gases ($\bar{\gamma} \sim 1.3$) or the bipropellant gases ($\bar{\gamma} \sim 1.22$). This value of ψ is lower than the values theoretically predicted from normal-shock theory as depicted in Fig. 3. Theoretical values of $\psi_{max} = 1.605$ and $\psi_{max} = 1.672$ would be obtainable for $\gamma = 1.3$ and $\gamma = 1.22$ respectively, using a nozzle with $\epsilon = 20.3$. It was found that configuration 2 with $\psi = 1.545$ could not be started with nitrogen for values of p_t/p_a up to 26, which was the upper limit of the available facilities.

The effect of second-throat length-to-diameter ratio L/D_d^* on the starting and operating characteristics of configuration 2 with $\psi = 1.545$ and $\bar{\gamma} \sim 1.3$ is shown in Fig. 16. These tests, however, were made using a shorter subsonic diffuser than that pictured in Fig. 2 for configuration 2. Although the minimum system pressure ratio for starting the diffuser does not appear to be a strong function of L/D_d^*, the converse is true for the minimum operating pressure ratio. Based on these results, $8 < L/D_d^* < 12$ was selected as the practical working range for subsequent tests on second-throat type diffusers, and no further optimization studies of this nature were conducted for later configurations or for other gases.

The performance of configuration 2 with two different gases is shown in Figs. 11 and 12. A comparison of these curves will show that this configuration using gases of $\bar{\gamma} \sim 1.3$ had a minimum operating pressure ratio less than this value when used with gases of $\bar{\gamma} \sim 1.22$. The cavity pressure p_b, however, was higher for a full-flowing nozzle when $\bar{\gamma} \sim 1.3$ gases were used than when $\bar{\gamma} \sim 1.22$ gases were used. Comparable curves for configuration 3 are shown in Figs. 13,

14 and 15 for three different gases. In these figures some rather striking differences in performance between the three gases are apparent. Configuration 3 had no performance hysteresis when used with $\bar{\gamma} \sim 1.22$, very small hysteresis when used with $\bar{\gamma} \sim 1.3$, but large hysteresis when used with $\gamma = 1.4$. Large differences are also evident in regard to the minimum starting and minimum operating regions of this configuration when used with the three gases. The lowest cavity pressure for a full-flowing nozzle was measured with nitrogen. When monopropellant gas products were used, the cavity pressure and nozzle exit pressure were nearly the same, but had a peculiar relationship by virtue of a cross-over effect. This condition may be observed in Fig. 14. At the lower values of p_t/p_a for which the nozzle flowed full, p_e/p_a was less than p_b/p_a. This result was never obtained with the other two gases. A comparison between configurations 2 and 3--for example, Fig. 14 with Fig. 11 or Fig. 13 with Fig. 12-- will show that configuration 2 required a considerably higher starting pressure ratio than did configuration 3 and also had a somewhat higher operating pressure ratio than configuration 3, although the latter effect was not so pronounced.

The static-pressure distributions measured at the wall of configuration 2 are shown in Fig. 17 for $\bar{\gamma} \sim 1.22$. The wall static-pressure distributions of configuration 3 for $\bar{\gamma} \sim 1.22$, $\bar{\gamma} \sim 1.3$, and $\gamma = 1.4$ are shown in Figs. 18, 19, and 20, respectively. The relation of the axial distance x/D_e to the diffuser area ratio A/A_e can be seen in Fig. 6. All these diffuser pressure distributions bear a family resemblance which is also similar to that of the constant-area-duct type diffuser shown in Fig. 10. In all cases for which the nozzle flows full, the axial location at which a rapid increase of static pressure occurs moves downstream

with increasing system pressure ratio. Physically this indicates that as the system pressure ratio is increased above the minimum starting point of a diffuser, smaller and smaller values of L/D_d^* are needed. By an inverse process of thinking it can be inferred that large values of L/D_d^* are associated with minimizing the operating point of a second-throat type diffuser. The result is confirmed by the experimental results shown in Fig. 16. It will be seen from Figs. 6, 17 - 20, that approximately 65 to 80 per cent of the static pressure that was recovered by the diffuser occurred in the second throat of configurations 2 and 3 at values of p_t/p_a near the minimum operating point. On the other hand, it is not obvious from Figs. 17 and 18 why configuration 3 has a lower starting pressure ratio than configuration 2. Configuration 2 might possibly contain a stronger shock train upstream of the second throat than configuration 3, which would result in a greater total pressure loss and reduced efficiency. Calculated values of efficiency for various test conditions are given in Tables 2 and 3.

3. Additional Observations on Second-Throat Type Diffusers

a. Diffuser cavity diameter

All experiments on model diffusers were made using the type of engine-diffuser coupling shown in Fig. 1a. The length of the cavity, the dimension a, was not varied during the experiments. This cavity was incorporated in the model configurations to simulate as closely as possible the expected conditions between the nozzle exit plane and the diffuser inlet of the full-scale engine-diffuser system. Certain beneficial results were obtained through the use of a cavity. Very early tests were made with configurations which had no cavity, i.e., with $D_b = D_e$, and

these tests indicated that there was a strong tendency for the nozzle flow to separate near the nozzle exit plane, even when the diffuser was started. This effect was sometimes noticed for constant-area-duct type diffusers when D_b/D_e=1.0 as well as for second-throat type diffusers. The presence of a cavity with $D_b > D_e$ eliminated this problem. A limited number of tests were made with configurations 2 and 3 using a reduced cavity diameter, with D_b/D_e = 1.065 rather than the value listed in Fig. 2a. The length of the cavity was not changed for these tests. The results indicated a slight improvement in the minimum operating pressure ratio for both configurations 2 and 3 with $\bar{\gamma} \sim 1.22$, but no change in the starting conditions was detected.

b. Diffuser entrance section

Additional experiments with configurations 2 and 3 included changing the angle θ and the length of the straight section upstream of the second throat. Both monopropellant and bipropellant gases were used in the following tests:

(1) Configuration 2, with θ = 5 deg

(2) Configuration 3, with θ = 7 deg

(3) Configuration 3, eliminating the straight section, with $\alpha = \theta$ = 5 deg (a continuous inlet contraction cone)

For test (1), little performance change was noted for θ = 5 deg compared with 3 deg, for $\bar{\gamma} \sim 1.3$. For tests (2) and (3), slight improvements in operating conditions were realized with these changes for $\bar{\gamma} \sim 1.3$; but no improvements and even detrimental changes were noted for $\bar{\gamma} \sim 1.22$. It was concluded that the marked improvement in performance, especially in the starting conditions, for configuration 3 as compared to configuration 2, was the effect of both shortening

the straight section and changing θ from 3 to 5 deg, not an effect due solely to one or the other of these changes. Configuration 3 as shown in Fig. 2 was selected as the optimum configuration for bipropellant testing with $\bar{\gamma} \sim 1.22$.

c. Subsonic cone angle and area ratio

During the course of the tests several subsonic diffusers were used interchangeably with various configurations, and no measurable differences in performance were noted among them. These tests were all made with $L/D_d^* = 10$. No systematic tests were made to determine the effect of θ, the half-angle of the subsonic diffuser, or of the effect of the subsonic diffuser area ratio, A_o/A_d^*, on diffuser performance. It is possible that the angle and area ratio of the subsonic diffuser may be of great importance for L/D_d^* less than 8.

d. Time interval

In testing second-throat diffusers, an effect of time interval upon the minimum starting and minimum operating characteristics was noted, especially with $\bar{\gamma} \sim 1.3$. The starting performance results given previously are quoted for a starting time of 5 sec or less. This is the time required, measured from initiation of gas flow, for the nozzle to flow full. It was found that for all configurations with $L/D_d^* = 10$ and $\bar{\gamma} = 1.3$ the system pressure ratio required for starting could be appreciably reduced if the starting time was allowed to increase. If the starting time was increased from 5 sec to as much as 30 sec, the starting value of p_t/p_a was correspondingly decreased by 10 to 13 per cent. Minimum operating results given in this paper were determined by a gradual decrease of p_t/p_a from the starting value. An effect of time on the minimum operating results was noted when the reduction from the starting point was done rapidly, i.e., of the order of

2 or 3 sec. For rapid reductions of the system pressure ratio, the minimum operating point was seen to increase by as much as 5 or 6 per cent.

The time effects just mentioned were small for bipropellant tests and almost negligible for nitrogen tests. The beneficial effect of time on the starting characteristics of diffusers is not recommended as a practical design factor for full-scale rocket-engine diffusers because the engine may not physically endure long durations of separated nozzle flow. On the other hand, to get the very best results from second-throat type diffusers, the reduction from starting to operating conditions should be accomplished in not less than approximately 5 sec.

e. Heat transfer

No attempt was made to determine heat-transfer rates or gas-side heat-transfer coefficients in any of the tests involving the use of the decomposition products of hydrazine or the combustion products of N_2O_4—N_2H_4. It should be pointed out that the direction of heat transfer in these two cases was from the gas to the diffuser wall. This was opposite from the direction of heat transfer in the nitrogen tests.

No cooling problems were encountered in the monopropellant tests for which uncooled parts were used. It was readily apparent from the bipropellant tests, however, that regions of high local heat flux can occur in second-throat type diffusers. These regions of high local heat flux may possibly be attributed to shock-wave boundary-layer interaction, or in some cases to the presence of axial gaps in the parts near critical locations. Several burnouts were suffered near the upstream end of the second throat when the nozzle was not flowing full. In some tests hot spots occurred at the downstream end of the second throat or

near the upstream end of the subsonic diffuser. Except for the case of unusually high local heat fluxes, the type of spray cooling shown in Fig. 5 was found to be very effective if care was taken to insure an even spray pattern. Several second-throat sections were fabricated with an annulus to test the feasibility of forced flow cooling in the second throat. In these tests vortex motion of the cooling water was accomplished by arranging the water inlets and outlets to maintain tangential or spiral flow through the cooling passage. Both the spray-cooling and the vortex-cooling methods were found to provide adequate cooling. Most of the problems associated with local hot spots were removed when the axial gaps between adjacent diffuser sections were eliminated.

f. Conical nozzles

Tests were made using configurations 2 and 3 with conical nozzles which had an expansion area ratio of 20.3. These tests were limited to $\bar{\gamma} \sim 1.22$. The performance results obtained in these tests are included in the summary of data given in Table 2. The performance of configuration 2 was poorer when a conical nozzle was used. The performance of configuration 3, however, was approximately the same for both nozzles. As expected, the nozzle-exit static-pressure ratio p_e/p_a, measured at the wall, was lower for the conical nozzle than for the contour nozzle. The cavity pressure ratio p_b/p_a was slightly higher for the conical nozzle as compared to the contour nozzle.

4. Auxiliary Methods of Starting and Operating Second-Throat Type Diffusers

a. Experiments conducted with a diffuser exhausting into a vacuum tank as a starting technique

The vacuum-tank experiments were made using configuration 2 with a short subsonic diffuser, $D_o/D_d^* = 1.422$, and $\bar{\gamma} \sim 1.3$. Two tank sizes were tested: nominal volumes of 4 and 50 cu ft. An arrangement of the apparatus is shown in Fig. 21. To prepare for an experimental test, a light-weight blow-off disk was placed on the downstream opening of the vacuum tank and the whole system was evacuated to the desired pressure level. After gas flow was initiated, the vacuum tank began to fill until atmospheric pressure was reached in the tank, at which time the blow-off disk fell away. During the time that pressure in the vacuum tank was increasing, before the disk fell away, the vacuum tank served as an auxiliary device for starting. Thereafter it was inoperative and did not affect the diffuser performance.

When the vacuum tank is not used, the minimum required starting values of the system pressure ratio, p_t/p_a, and the static pressure ratio across the diffuser, $(p_b/p_o) = (p_b/p_a)$, are uniquely related. If the diffuser ambient pressure is reduced during the starting transient by means of a vacuum tank, then $p_o = p_T < p_a$. The cavity pressure would then be reduced so that $p_b < p_o$, and the diffuser pressure ratio p_b/p_o would be approximately the same as in tests without a tank. The nozzle-exit static pressure is also reduced because of its relationship with the cavity pressure, so that for a given nozzle pressure ratio of p_e/p_t, based on nozzle area ratio, the minimum starting total pressure should also be reduced. In other words, the use of a vacuum tank should allow the diffuser to start at a system pressure ratio p_t/p_a lower than that required when no tank is used. The effectiveness of this vacuum tank technique probably hinges on the rates of change with time of the diffuser-exit static pressure p_o and the static

pressure in the vacuum tank p_T. If these rates are too rapid and the vacuum tank pressure increases too rapidly, the nozzle may not have the opportunity to flow full at a lower starting pressure. These factors can be controlled to some extent by the volume of the tank and the initial level of the tank pressure acquired by evacuation.

Table 5 shows the best results obtained with the two tanks previously mentioned. It is clear from these results that the small tank reduced starting pressure slightly and that the large tank reduced starting pressure substantially. At full scale these tank sizes would be very large, and it is questionable whether they would be practical. Attempts to improve the starting characteristics of any of the configurations by placing a blow-off disk on the diffuser itself and pre-evacuating the nozzle and diffuser system did not reduce starting pressure since the diffuser itself did not have adequate volumetric capacity. The best results obtained with the large tank are included in the summary of Table 3 and also in Fig. 7.

b. Experiments conducted using annular ejection of a secondary gas at the exit of the subsonic diffuser

An attempt to improve both the starting and the operating performance of configuration 2 was made by using annular ejection of high-pressure nitrogen gas at the exit of the subsonic diffuser. A schematic arrangement of the test apparatus is shown in Fig. 22. Nitrogen was introduced through an annular sonic nozzle and the combined mixture of the primary gas--in this case the decomposition products of hydrazine--and the secondary gas, then flowed through a mixing duct and discharged into the atmosphere. The ratio of the secondary weight rate of flow to the primary weight rate of flow could be varied from zero to approximately 4.5 with the available equipment.

With the ejector, the exhaust gases from the diffuser are accelerated by the ejection of the secondary gas, at least in the vicinity of the wall, and the exit static pressure of the diffuser is thereby reduced. By the same arguments advanced in the previous section on the use of a vacuum-tank start, the minimum system pressure ratio for starting should be reduced by reducing diffuser ambient or exit pressure. If the ejector operation is continued during diffuser operation, the minimum system pressure ratio for operation should also be reduced.

It was found that the diffuser could not be started if the secondary flow was initiated before the primary flow; consequently, it became necessary to initiate the primary flow before starting the ejector. The ejector did not improve the starting performance of the diffuser, but a considerable reduction in the operating pressure ratio was achieved for large secondary weight rates of flow. Figure 23 shows a plot of the effect of secondary flow on the minimum operating system

pressure ratio. The best results that were obtained are also shown in Table 3. Note that rather large secondary flow rates were required to achieve this benefit. Tests made with ratios of mixing-duct length to diameter of L_E/D_E = 6, 8.1, 10.1, and 11.3 did not alter the results.

Perhaps one reason can be ascribed to the inability of the ejector located at the diffuser exit to improve the starting performance of the diffuser. If for some reason flow separation occurred in the subsonic diffuser during the starting transient, the core of the separated wake would scarcely be accelerated by nitrogen ejection of the type used. Another ejector, however, was designed to test the feasibility of introducing secondary gas into the core of the primary flow rather than at the wall. Here nitrogen ejection was accomplished by means of a streamlined center body located at the exit of the subsonic diffuser. This ejector, when tried with configuration 3 and $\bar{\gamma} \sim 1.3$, did not help or hinder the performance in any way for either the starting or operating conditions. Unfortunately, this ejector was never tested with configuration 2.

Another ejector which was designed to introduce nitrogen gas through an annular supersonic nozzle into the primary flow at a location near the nozzle exit plane was unsuccessful. The diffuser could not be started regardless of the amount of secondary flow or of the starting sequence of the ejector, that is, before or after the initiation of primary flow. This ejector was used with configuration 2 and $\bar{\gamma} \sim 1.3$.

Nitrogen gas at $T_t \sim 480°R$ has a rather high molecular weight to be used for an ejector in conjunction with decomposition products of hydrazine; however, it was conveniently available.

c. Experiments conducted using primary-gas extraction near the entrance of the second throat

Theoretically, the minimum operating point of a second-throat type diffuser could be reduced if the second throat were made smaller than that required to start the diffuser. One method of accomplishing this would be to employ a variable-throat-area diffuser. This type of design would require considerable ingenuity for an axisymmetric diffuser or would impose severe cooling problems if a retractable center body were used. A second approach to the problem would be to use a smaller second throat than the starting limitation would permit and to start the diffuser by auxiliary means. One practical means of accomplishing this is presented in references (8) and (9) and was adopted for these tests. Mass extraction is applied during the starting transient at a location upstream of the second throat. Primary gas is extracted from the diffuser at this location through an annular suction slot and then passes into a vacuum tank. The vacuum tank must be large enough so that the diffuser will have started before the vacuum-tank pressure has reached the level of the diffuser wall pressure at the slot location. The effect of the mass extraction, or bleed, on starting is a reduction of the mass flow per unit cross-sectional area at the diffuser throat, thereby providing an effective second throat larger than the geometrical value.

Figure 24a shows a sketch of configuration 3A which is identical to configuration 3 except that the diffuser throat area has been reduced by 12.1 per cent, the contraction ratio increased from 1.545 to 1.758, and an annular suction slot installed upstream of the entrance to the second throat perpendicular to the diffuser axis. The downstream edge of the slot was located at ψ = 1.545, which was

the contraction area ratio used for configuration 3. A schematic arrangement of the test apparatus is shown in Fig. 24b. With the pneumatic valve in the closed position the tank was evacuated to the desired pressure level using a vacuum pump. The pump was then shut off just prior to a test. The pneumatic valve was opened simultaneously with the initiation of the primary flow, allowing gas to bleed into the tank. Flow into the vacuum tank ceased when the static pressure in the vacuum tank equaled the local static pressure in the diffuser at the slot location. In these tests steady-state pressure in the vacuum tank was reached in less than 1 sec. For all tests the initial pressure in the vacuum tank was 0.1 psia or less and all tests were made using the combustion products of N_2O_4—N_2H_4. It had been expected that severe heating and possible melting of the downstream edge of the suction slot would occur on bipropellant tests; however, except for slight discoloration of this edge, no serious problem arose during the tests from this cause.

Two tank sizes were tested with configuration 3A: the nominal volumes were 1 and 4 cu ft. The manifold and piping system used to connect the vacuum tanks to the diffuser had a volume of approximately 20 per cent and 6 per cent of the volume of the small and large tank respectively. The performance of configuration 3A used with the larger of the two vacuum tanks is shown in Figs. 7, 8, and 13 and in Table 3. Note that the starting performance was the same as for configuration 3, but that the operating point was decreased by approximately 18 per cent. Also shown in Fig. 13 are experimental points obtained using configuration 3A without the vacuum tank. In this case the diffuser definitely could not be started. Table 6 shows the effect of tank size on the performance of configuration 3A.

A second suction slot was designed for use with configuration 3 modified to have an even greater contraction ratio of $\psi = 2.017$. This slot was inclined 40 deg to the diffuser axis instead of 90 deg, and had a sharp downstream edge. The slot had slightly diverging walls. It was found that this diffuser arrangement could not be started. It is likely, however, that choked flow conditions occurred in the manifold system with the result that the rate of mass extraction on starting was insufficient to accomplish the purpose. The sharp downstream edge of this slot melted during the course of these experiments. It has not been concluded that configuration 3 with $\psi = 2.017$ will not start, but further tests would be needed to establish the possibility of using so large a contraction ratio.

5. The Performance of a Canted Diffuser to Simulate Nozzle Gimballing

In order to test the possible effects of gimballing an engine on the performance of a second-throat type diffuser, configuration 3 was modified so that wedges could be inserted between the nozzle exit and the diffuser inlet section. Such an arrangement is shown in Fig. 25. Wedge angles β of 3, 5, and 7 deg were tested. Since this type of test allows a particular but fixed angle of misalignment between the nozzle center line and the diffuser center line for each wedge inserted, it is not truly representative of the dynamic angular change which would occur in an engine gimballing test. The test is nevertheless indicative of the performance of diffusers canted with respect to the nozzle. These tests were made using the combustion products of nitrogen tetroxide and hydrazine only.

The effect of wedge angle on diffuser performance is shown in Fig. 26. As expected, the minimum system pressure ratio required for starting increases with

increasing wedge angle. Strangely, the minimum system pressure ratio for operation is reduced for moderate wedge angles. The reason for the latter phenomenon is not apparent. None of the changes in performance was large, however, for either starting or operating.

The diffuser was spray-cooled for all these tests. During the course of these experiments considerable care had to be exercised to insure that burnouts would not occur in the second throat on the side of the wall inclined in the direction of the nozzle axis. The opposite side of the second-throat wall which was inclined away from the nozzle axis presented no cooling problem. Water-coolant sprays were carefully directed to impinge on critical locations on the outside of the diffuser wall. Nevertheless, burnouts were narrowly averted in several instances. The position of the hot spots generally moved upstream with increasing wedge angle.

THE FULL-SCALE DIFFUSER

The nominal diametrical scale factor between the model diffuser and the full-scale diffuser is ten. The full-scale diffuser is modelled after configuration 2 with some minor alterations. A sketch of the vacuum chamber, which contains the engine, and the diffuser is shown in Fig. 27. Note that the engine and the diffuser are not mechanically coupled but rather that the diffuser is attached to the vacuum chamber. The diffuser itself is composed of five axisymmetric double-walled sections which are fastened together by means of bolted flanges. Sections of the inner liner were rolled from 0.25-in.-thick, type 321 stainless-steel sheet stock and arc-welded longitudinally. The welds were ground to give a smooth inner contour on the gas side. Sections of the outer shell were made from

standard mild steel pipe having a wall thickness of 0.375 in. The flanges of the inner liner and the outer shell were purposely staggered to facilitate assembly. An expansion joint located in the first section of the second throat allows the outer shell to expand together with the inner liner. The diffuser was found to experience an over-all thermal expansion of approximately 0.70 in. during engine tests. A distance of approximately 0.5 to 1.0 in. was allowed between the nozzle exit plane and the upstream side of the vacuum chamber flange when an engine was installed. The vacuum chamber flange just mentioned was fitted with a cooling ring to prevent it from being burned by the exhaust gases of the engine.

Each of the five sections of the diffuser was provided with a separate cooling passage which was formed by the annular space between liner and outer shell. Cooling water was introduced into each passage by four nozzles at both ends of each diffuser section and removed by a single outlet centrally located at the top of each section. The inlet nozzles were arranged so that water was introduced tangentially into the passages, thereby imparting a spiral or vortex motion to the cooling water. As indicated by Fig. 27, the diffuser was supported by cradles fitted with rollers. These rollers and their guide rails are shown in Fig. 28, which is a photograph of the exit end of the diffuser.

Included in Fig. 27, but not shown in the photograph, is the hinged lid serving to cover the diffuser exit when desired. The purpose of this lid was twofold: (1) to allow vacuum starts of the engine for vacuum-ignition studies and (2) to reduce the large pressure and thrust overshoot that had been experienced by the engine on start. When the diffuser is started without the lid, the column of air contained in the diffuser must be removed very rapidly by the engine exhaust

gases. The resulting shock-type impact between the gases may have accounted for a large pressure overshoot which occurred in the vacuum chamber before use of the lid became standard operating procedure. When the lid is used, the diffuser and vacuum chamber are evacuated to a low pressure before the engine is started, and then the lid is blown open by the momentum of the engine exhaust gases during the starting transient. Measurements have indicated that the lid begins to open approximately 40 millisec after engine ignition. During engine shutdown a reversal of the phenomenon described above causes a similar pressure overshoot in the vacuum chamber.

Instrumentation was installed in the diffuser not only to judge the performance of the diffuser but also to warn of possible trouble during engine tests. Most of the engines tested were provided with one or more static-pressure taps at the nozzle exit. Pressure readings obtained from this tap, together with readings obtained from a pressure tap located in the vacuum-chamber flange immediately downstream of the cooling ring, served to indicate whether or not the diffuser had started and whether or not the nozzle was flowing full. Three thermocouples located in the wall of the second throat, as shown in Fig. 27, served to indicate an approximate value of the local gas-side wall temperature. Thermocouples installed in each of the water-coolant outlets indicated the coolant temperature rise across each of the respective diffuser sections. In addition, static-pressure taps were located in all water inlet and outlet piping. Readings from all the instrumentation were recorded during engine tests. Steady-state gas-side wall temperatures in the second throat ranged from 420° F to 900° F.

The starting and operating performance of this diffuser exceeded all expectations and predictions based on the bipropellant tests conducted on model configuration 2. The best performance of the diffuser to date is given in Table 7. This diffuser has been operated at pressure ratios up to $p_t/p_a = 18$. The minimum starting and operating points of the diffuser have not been absolutely determined, but the values listed in Table 7 are believed to be near the minimum values. If the results shown in Table 7 are compared with the model results shown in Fig. 12, it will be noted that the full-scale-diffuser starting and operating system pressure ratios are substantially lower than corresponding values obtained on the model tests.

CONCLUSIONS

Exhaust diffusers, which utilize the momentum of the exhaust gases of rocket engines, are one type of device that is capable of reducing engine back pressure sufficiently to allow supersonic nozzles of large expansion area ratios to flow full at ground level under certain conditions. The advantages of exhaust diffusers are their practicality, simplicity, and low cost; however, they have the disadvantage that they are not readily adaptable to engines of different size.

Unfortunately, the design of supersonic diffusers, especially for use with rocket engines, presents problems which can be solved only by the application of experience and experimental data. Even with experimental data available on models, the designer faces uncertainties when applying this information to the design of a larger configuration. Simple, one-dimensional, normal-shock theories are widely used as a basis for judging diffuser performance but are not really adequate for design purposes.

The results of a model diffuser program using fixed-geometry, axisymmetric configurations with three different gases and no auxiliary equipment indicated the following:

1. Constant-area-duct type diffusers are inadequate to meet the requirements of a 20:1-expansion-ratio nozzle operating at 150-psia chamber pressure.
2. The operating point for the best second-throat type diffuser tested exceeded the design chamber pressure of the engine by 8 to 9 per cent when gases with $\bar{\gamma} \sim 1.22$ were used.
3. Second-throat type diffusers gave the best performance when the length-to-diameter ratio of the second throat was larger than 8.
4. The maximum allowable contraction area ratio for starting second-throat type diffusers was determined to be the same for three gases having a γ variation between 1.22 and 1.4. For $\bar{\gamma} = 1.4$, this ratio exceeded the maximum predicted by less than 1 per cent, and for $\bar{\gamma} \sim 1.3$ and $\bar{\gamma} \sim 1.22$ it was less by 3.7 and 7.6 per cent, respectively, than the maximum predicted.
5. For second-throat type diffusers the configuration of the diffuser preceding the second throat has a profound effect on the performance, especially on the starting point.
6. Temperature and γ effects of gases having widely varying properties are not only significant but unpredictable, even when these gases are used with exactly the same diffuser configuration.

7. Regions of high local heat flux can exist in second-throat type diffusers used with rocket engines.
8. Second-throat type diffusers can be successfully cooled by external water sprays or forced convection cooling applied to the outer surfaces of the diffuser.
9. For the same nozzle-expansion-area ratio and the same configuration, diffusers used with a contour nozzle exhibited somewhat better performance than diffusers used with a conical nozzle.
10. The best second-throat type diffuser tested suffered little or no performance loss with an angular misalignment between the nozzle and diffuser axes up to 7 deg when used with the combustion products of N_2O_4—N_2H_4.

Various techniques for improving the starting and the operating performance of second-throat type diffusers were investigated. Such techniques involved the use of auxiliary equipment in conjunction with a diffuser. The results of these experiments indicated that:

1. The use of secondary mass injection at the diffuser exit is not practical because of the large amount of secondary mass flow needed.
2. Vacuum-tank starts, during which the entire gas flow passes through the diffuser and then discharges into a vacuum tank, are not practical because of the prohibitively large tank volume that is needed.
3. Extraction of primary gas during starting at the entrance to the second throat, which allows the use of a second throat of smaller area than

possible without gas extraction, is a promising and practical method of improving the operating performance of a diffuser.

During the course of the model diffuser program many occasions arose when the cavity pressure, or diffuser-inlet static pressure, was sufficiently low that the nozzle should have flowed full, but did not. For this reason it is recommended that rocket-engine tests made with an exhaust diffuser should be accompanied by measurements of the nozzle-exit static pressure in order to verify that the nozzle is actually flowing full.

A substantial difference in starting and operating performance may exist between full-scale and model versions of a second-throat type exhaust diffuser. Differences in performance were exhibited by the results obtained from this type of diffuser when used with a 6000-lb-thrust, 20:1-expansion-area-ratio engine, as compared with results obtained on nominal tenth-scale models.

NOMENCLATURE

a = length of cavity following nozzle exit plane, in.

A = area, $in.^2$

D = diameter, in.

f = width of suction slot, in.

g = gravitational constant, 32.2 ft/sec^2

h = enthalpy, Btu/lb

J = constant, 778 ft-lb/Btu

K = coefficient in weight flow equation (see Appendix A)

L = axial length, in.

m = molecular weight, lb/lb mole

M = Mach number

p = static or total pressure, psia

R = gas constant, ft-lb/lb°R

T = static or total temperature, °R

v = velocity, ft/sec

V = volume, ft^3

$\dot{w}$ = weight rate of flow, lb/sec

x = axial distance from nozzle exit plane, in.

α, θ = diffuser contraction half-angles, deg

β = wedge angle (for simulated nozzle gimballing), deg

$\gamma, \bar{\gamma}$ = ratio, or average ratio, of specific heats

ϵ = nozzle-expansion-area ratio, A_e/A_n^*

η = efficiency

ρ = density of gas, lb/ft^3

ϕ = subsonic-diffuser expansion half-angle, deg

ψ = diffuser contraction ratio, A_e/A_d^*

Subscripts and Superscripts

a = ambient = atmospheric

b = cavity or region of base pressure

d = diffuser

e = nozzle exit

E = ejector mixing duct

n = nozzle

o = diffuser exit or exit to subsonic diffuser

p = primary gas

r = cooling ring (applies to full-scale diffuser only)

s = secondary gas when used with $\dot{w}$, normal shock when used with η, straight section when used with D

t = total or stagnation conditions

T = vacuum tank

v = vacuum chamber (applies to full-scale diffuser only)

x = conditions upstream of normal shock

y = conditions downstream of normal shock

max, min = maximum and minimum respectively

* = critical diameter or area, as nozzle or diffuser throats

Table 1. Gas properties and flow parameters used in experiments

Gas	$\bar{\gamma}$	T_t, °R	m	One-dimensional isentropic flow		Axisymmetric isentropic flow
				p_e/p_t [1]	M_e [1]	p_e/p_t [2]
Combustion products of hydrazine and nitrogen tetroxide	1.22 [3]	5000 [3]	19.3 [3]	0.00466	3.85	0.00636
Decomposition products of hydrazine	1.3 [4]	2110 [5]	12.8 [4]	0.00357	4.22	0.00486
Nitrogen gas	1.4	480 [5]	28.0	0.00256	4.74	0.00352

[1] Tabular values for $\epsilon = 20.3$

[2] Estimated values for $\epsilon = 20.3$, $p_t = 150$ psia (p_e at the wall) with contour nozzle

[3] Estimated for $p_t = 150$ psia and mixture ratio = 1.0

[4] Estimated for $T_t = 2110°R$

[5] Measured average values

Table 2. Average experimental performance of various model exhaust diffusers, without auxiliary equipment

Model diffuser configuration	Type nozzle[1]	$\frac{-}{\gamma}$	Minimum starting condition p_t/p_a	Minimum operating conditions				
				p_t/p_a	p_e/p_t	p_e/p_a	p_b/p_a	η_d
1 2	Contour	1.3	16.1	16.1	0.00497	0.080	0.100[5]	0.313
2 3	Contour	1.3	15.7	10.7	0.00467	0.050	0.040	0.415
2 4	Contour	1.22	15.6	12.0	0.00542	0.065	0.028	0.457
2 3	Conical	1.22	16.5	12.3	0.00642	0.079	0.064	0.406
3 4	Conical	1.22	11.7	11.7	0.00400	0.047	0.043	0.436
3 4	Contour	1.22	11.5	11.5	0.00670	0.077	0.035	0.451
3 4	Contour	1.3	10.4	9.75	0.00380	0.037	0.045	0.343
3 4	Contour	1.4	15.7	10.1	0.00347	0.035	0.015	0.424

[1]Nozzle-expansion-area ratio for all nozzles, $\epsilon = 20.3$; nozzle throat diameter for all nozzles $D_n^* = 0.552$ in.

[2]Constant-area-duct type diffuser with $D/D_e = 1.007$, $L/D = 13.6$

[3]Second-throat type diffuser, with $D_o/D_d^* = 1.422$

[4]Second-throat type diffuser as shown in Fig. 2

[5]Estimated value

Table 3. Average experimental performance of various model exhaust diffusers, with auxiliary equipment

Diffuser configuration and type of auxiliary equipment	Type nozzle	$\frac{-}{\gamma}$	Minimum starting condition p_t/p_a	Minimum operating conditions	
				p_t/p_a	η_d
2, with $D_o/D_d^* = 1.422$ vacuum-tank start with $V_T \sim 50$ ft^3	Contour	1.3	12.1	10.7	0.415
2, with $D_o/D_d^* = 1.358$ nitrogen ejector with $D_E/D_o = 1.012$, $L_E/D_E = 4.16$	Contour	1.3	15.7	8.75[1]	Not applicable
3A, with mass extraction on start, using annular suction slot, $\psi = 1.758$	Contour	1.22	11.5[2]	9.45[2]	0.494

[1] At a ratio of secondary to primary flow rate $\dot{w}_s/\dot{w}_p = 4.40$

[2] Using a vacuum tank plus manifold and piping volume of approximately 4.25 ft^3

Table 4. Results obtained with constant-area-duct type diffusers with $\bar{\gamma} \sim 1.3$ and contour nozzle with $\epsilon = 20.3$

D/D_e	L/D	$(p_t/p_a)_{min}$		$(p_e/p_a)_{min}$	
		Measured	Computed [1]	Measured	Computed [1]
1.007	11.6	16.2	14.3	0.0800	0.0516
1.007	13.6	16.1	14.3	0.0790	0.0516
1.007	19.6	15.6	14.3	0.0770	0.0516
1.110	5.1	20.5	17.3	0.0830	0.0626
1.110	12.4	19.1	17.3	0.0790	0.0626
1.110	17.8	19.0	17.3	0.0790	0.0626

[1]Using an approximate one-dimensional flow theory. These parameters are a function of γ, ϵ, and A/A_e only.

Table 5. Best results obtained with a vacuum-tank start using configuration 2 with $\bar{\gamma} \sim 1.3$, contour nozzle, $\epsilon = 20.3$

	No vacuum tank	Small vacuum tank	Large vacuum tank
V_T/A_n^* in^3/in^2	0	29,200	365,000
Initial evacuation pressure in tank p_T/p_a, atm	Not applicable	0.045	0.480
System pressure ratio for minimum start, p_t/p_a	15.7	14.5	12.1

Table 6. Performance results obtained with mass extraction on start, configuration 3A, $\bar{\gamma} \sim 1.22$

	Small vacuum tank	Large vacuum tank
V_T/A_n^* [1] in^3/in^2	8,250	31,000
System pressure ratio for minimum start, p_t/p_a [2]	12.5	11.5
System pressure ratio for minimum operate, p_t/p_a [2]	9.45	9.45

[1] V_T includes volume of manifolds and piping system

[2] Initial evacuation pressure $p_T \leq 0.10$ psia

Table 7. Best results obtained with the full-scale exhaust diffuser

Diffuser used with a 6000-lb-thrust rocket engine
and the combustion products of N_2O_4--N_2H_4.
Nozzle-expansion-area ratio ϵ = 20.0

Starting condition p_t/p_a	Operating conditions				
	p_t/p_a	p_e/p_t	p_e/p_a	p_b/p_a	η_d
12.7	10.3	0.00424	0.0437	0.0380	0.461

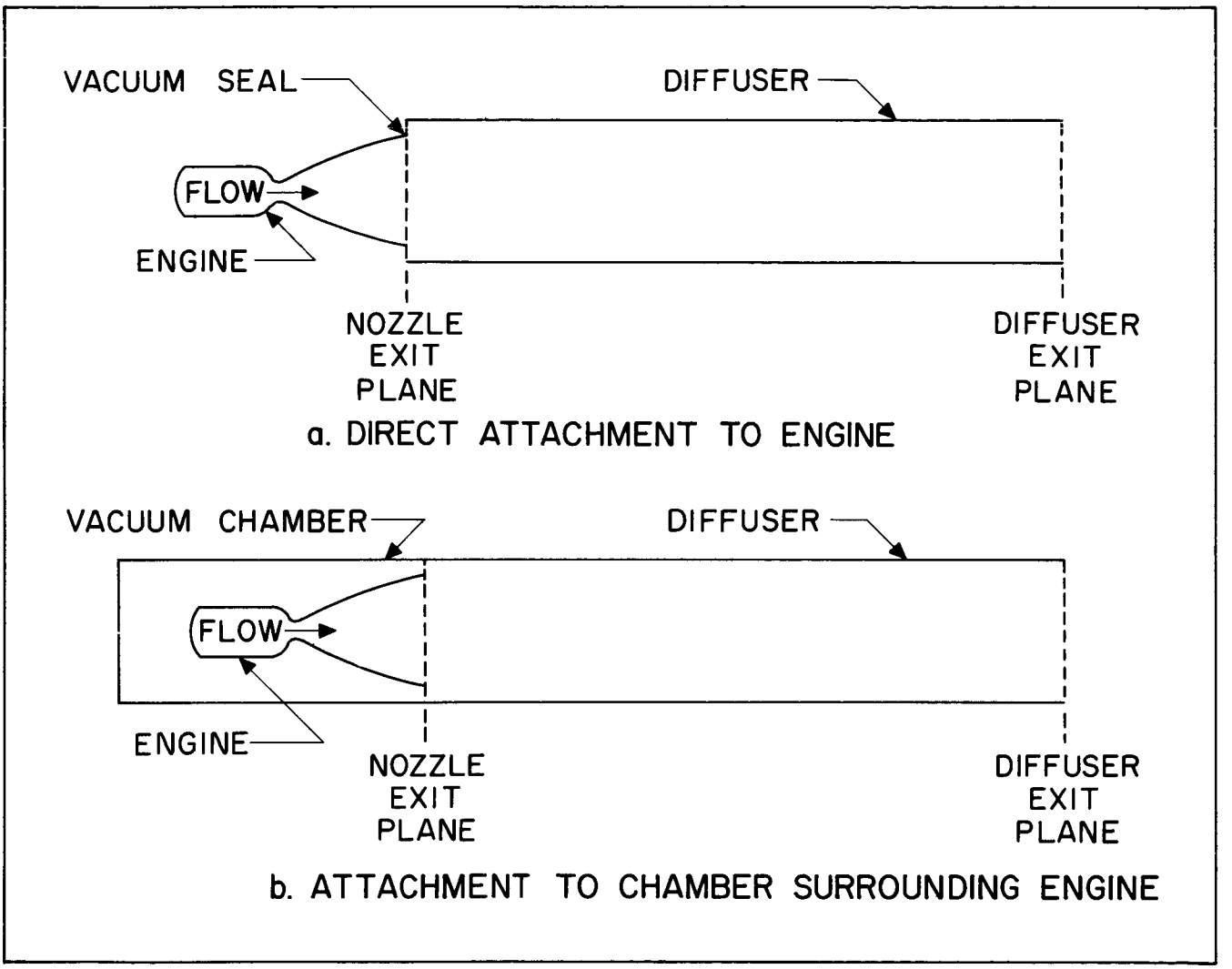

Fig. 1. Methods of adapting exhaust diffusers to rocket engines

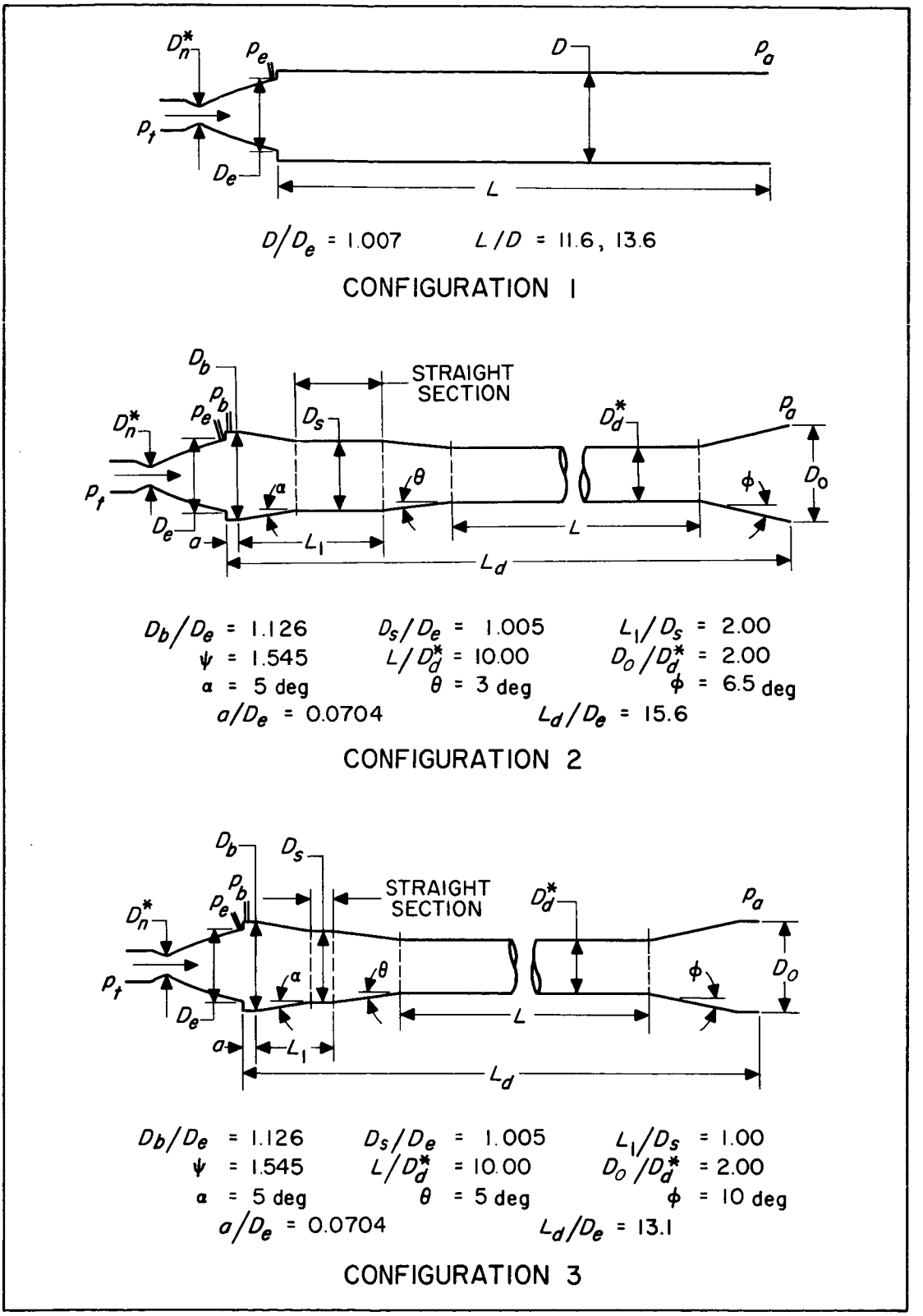

Fig. 2. Experimental diffuser configurations

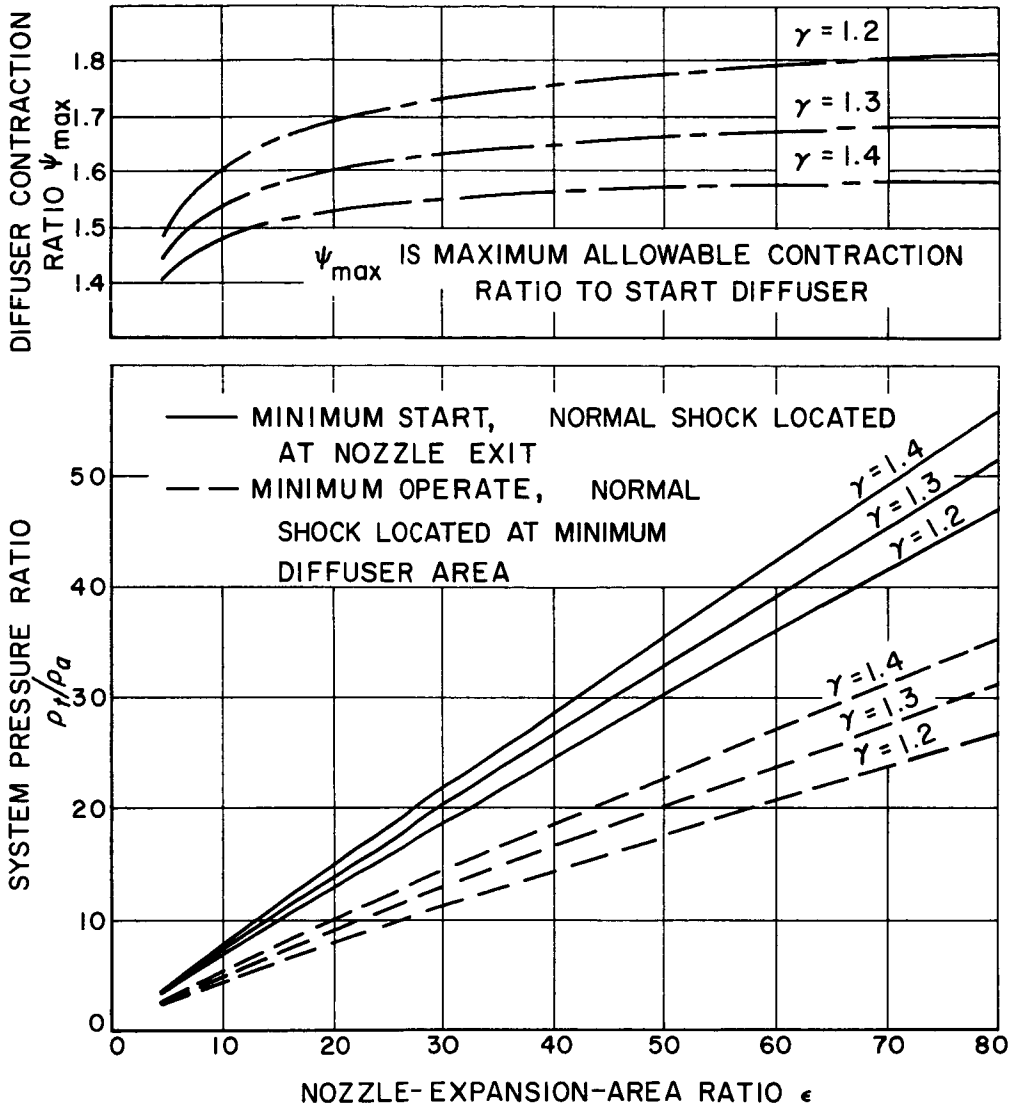

Fig. 3. Theoretical nozzle-diffuser performance based on one-dimensional, normal-shock flow theory

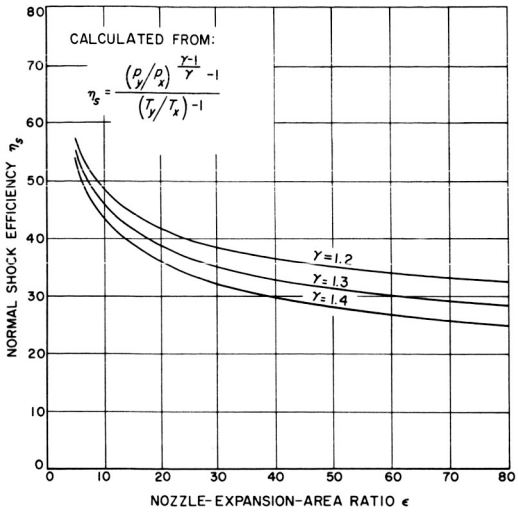

Fig. 4. Efficiency of a normal shock located at the nozzle exit

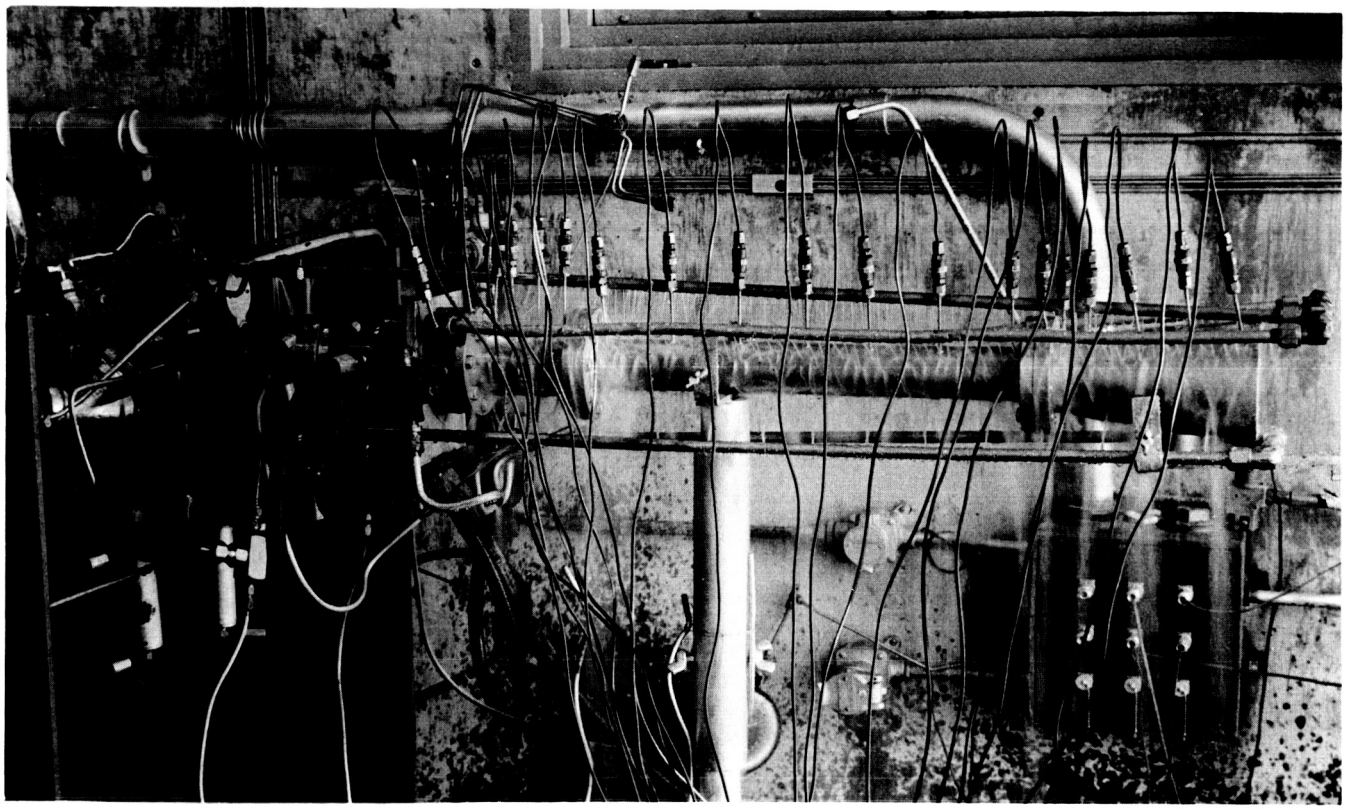

Fig. 5. External view of a typical model exhaust diffuser of second-throat type, showing method of spray cooling

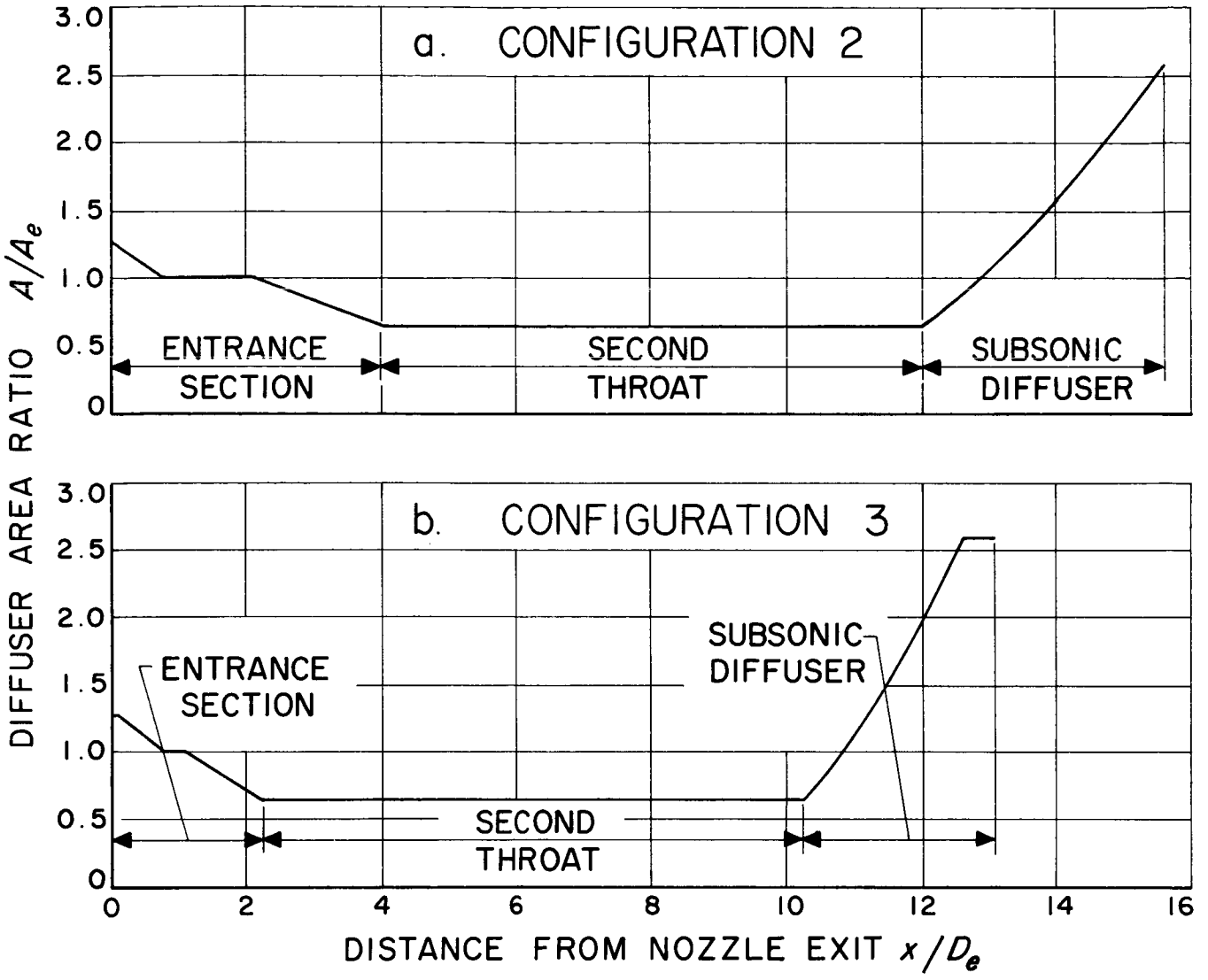

Fig. 6. Diffuser area ratio as a function of distance from nozzle exit

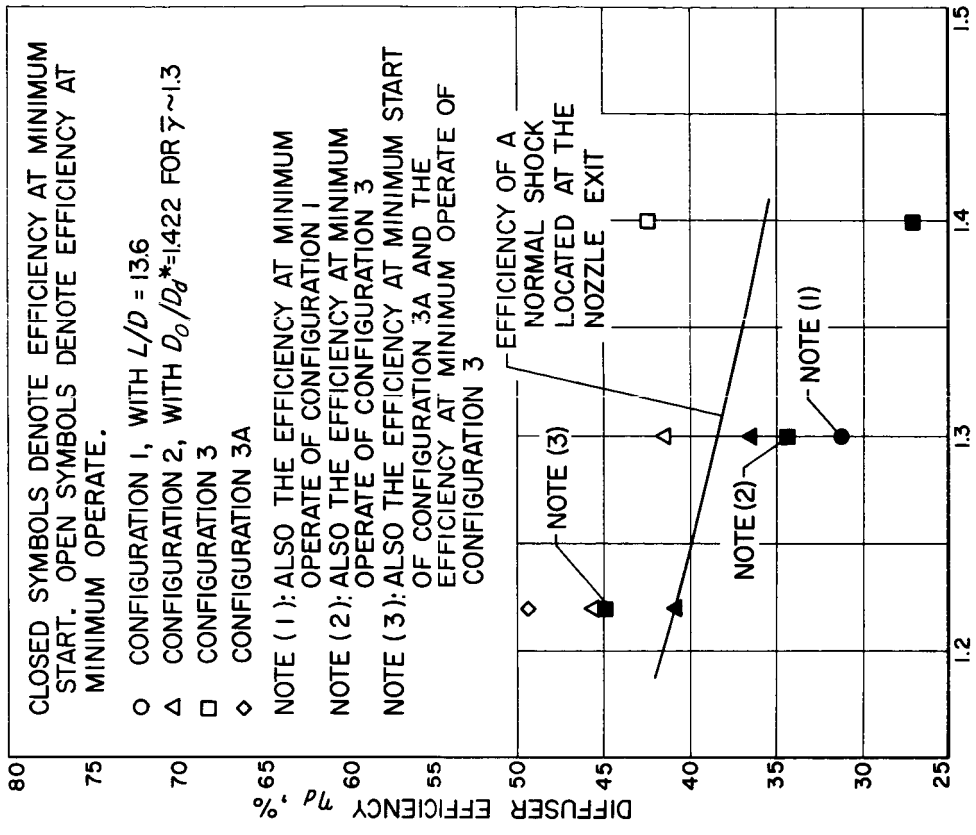

Fig. 8. Calculated efficiencies for model exhaust diffusers used with a contour nozzle, ϵ = 20.3

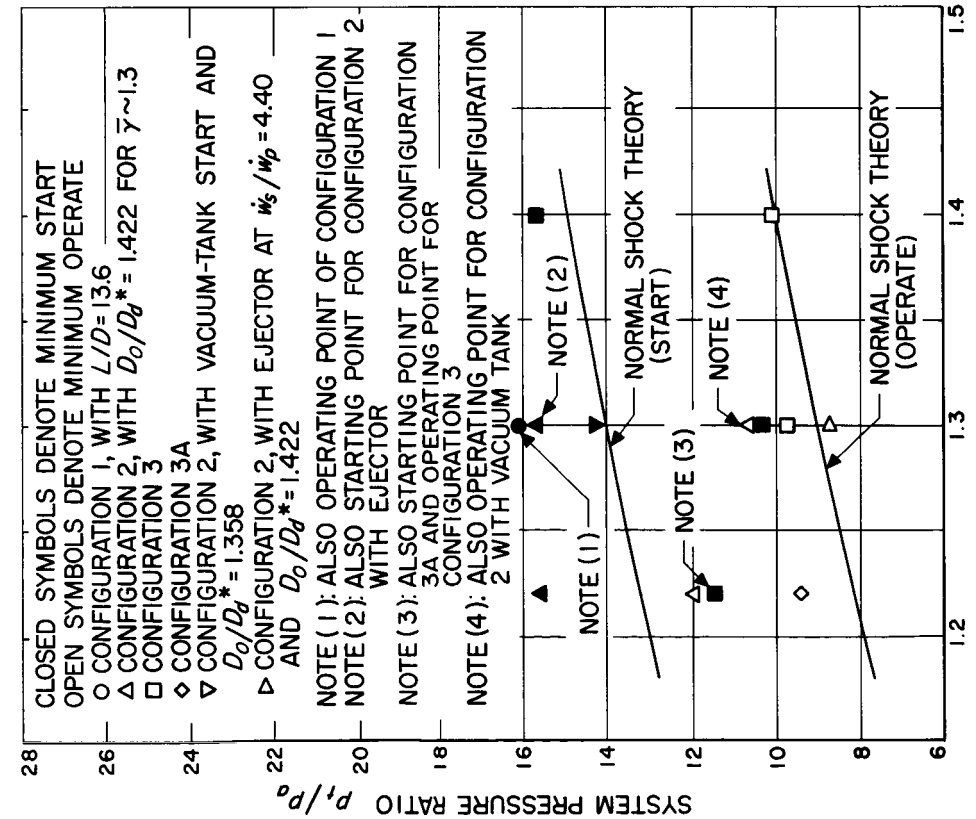

Fig. 7. Average experimental values for minimum starting and operating system pressure ratios; for model exhaust diffusers used with a contour nozzle, ϵ = 20.3

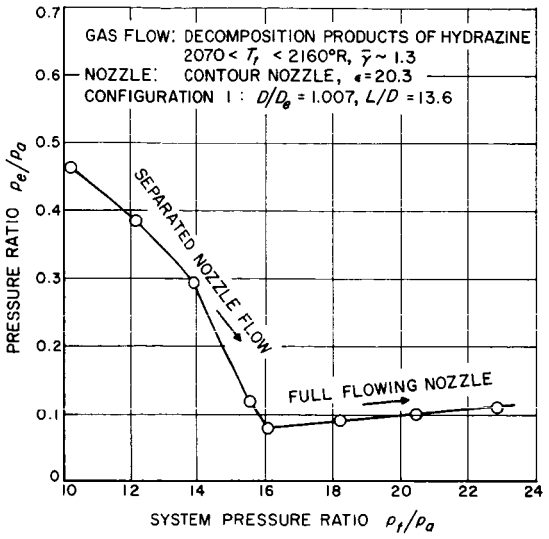

Fig. 9. Typical exhaust-diffuser performance, constant-area-duct type diffuser

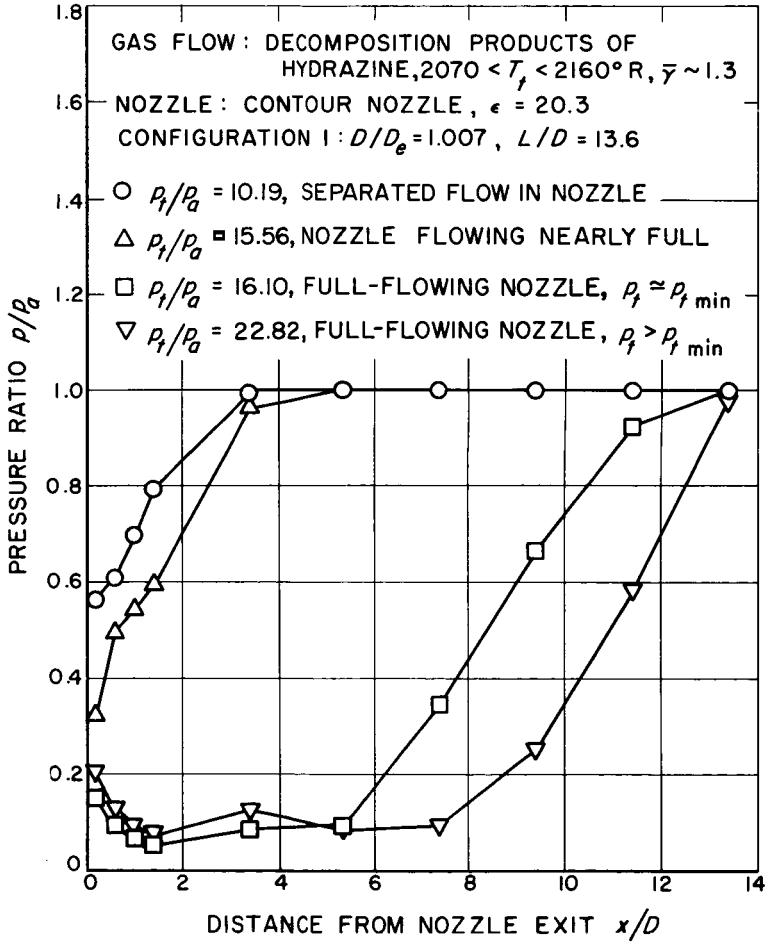

Fig. 10. Typical static-pressure distribution at the wall, constant-area-duct type diffuser

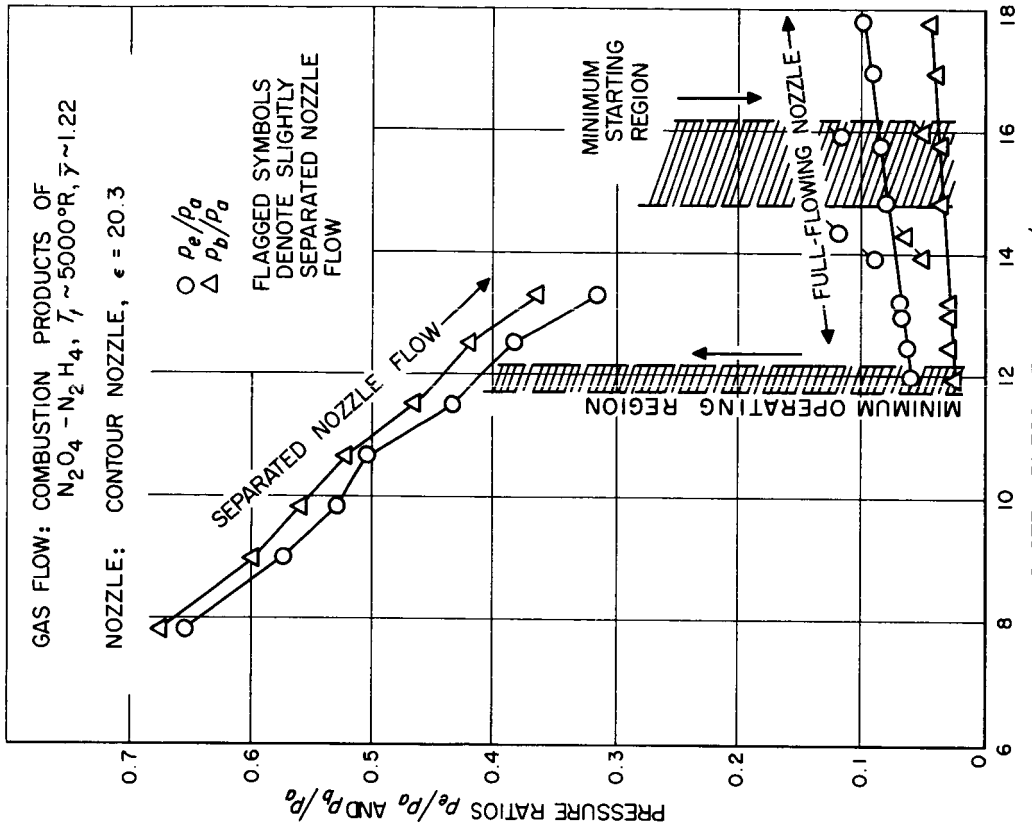

Fig. 12. Typical exhaust-diffuser performance, second-throat type diffuser, configuration 2, $\bar{\gamma} \sim 1.22$

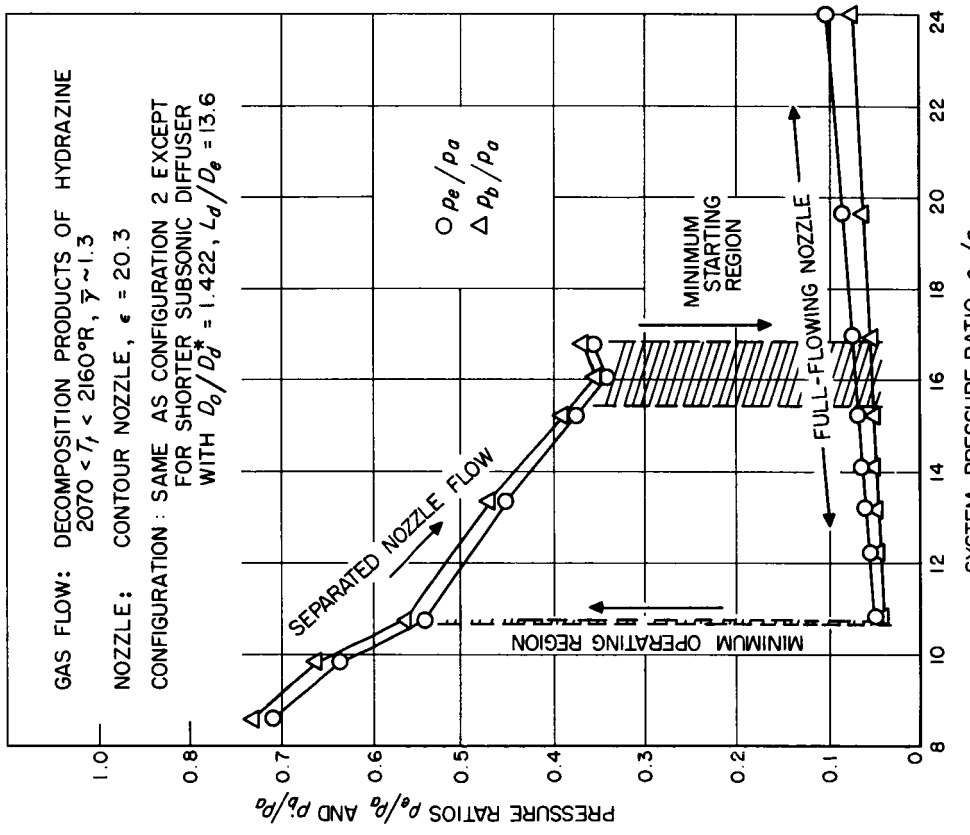

Fig. 11. Typical exhaust-diffuser performance, second-throat type diffuser, configuration 2, $\bar{\gamma} \sim 1.3$

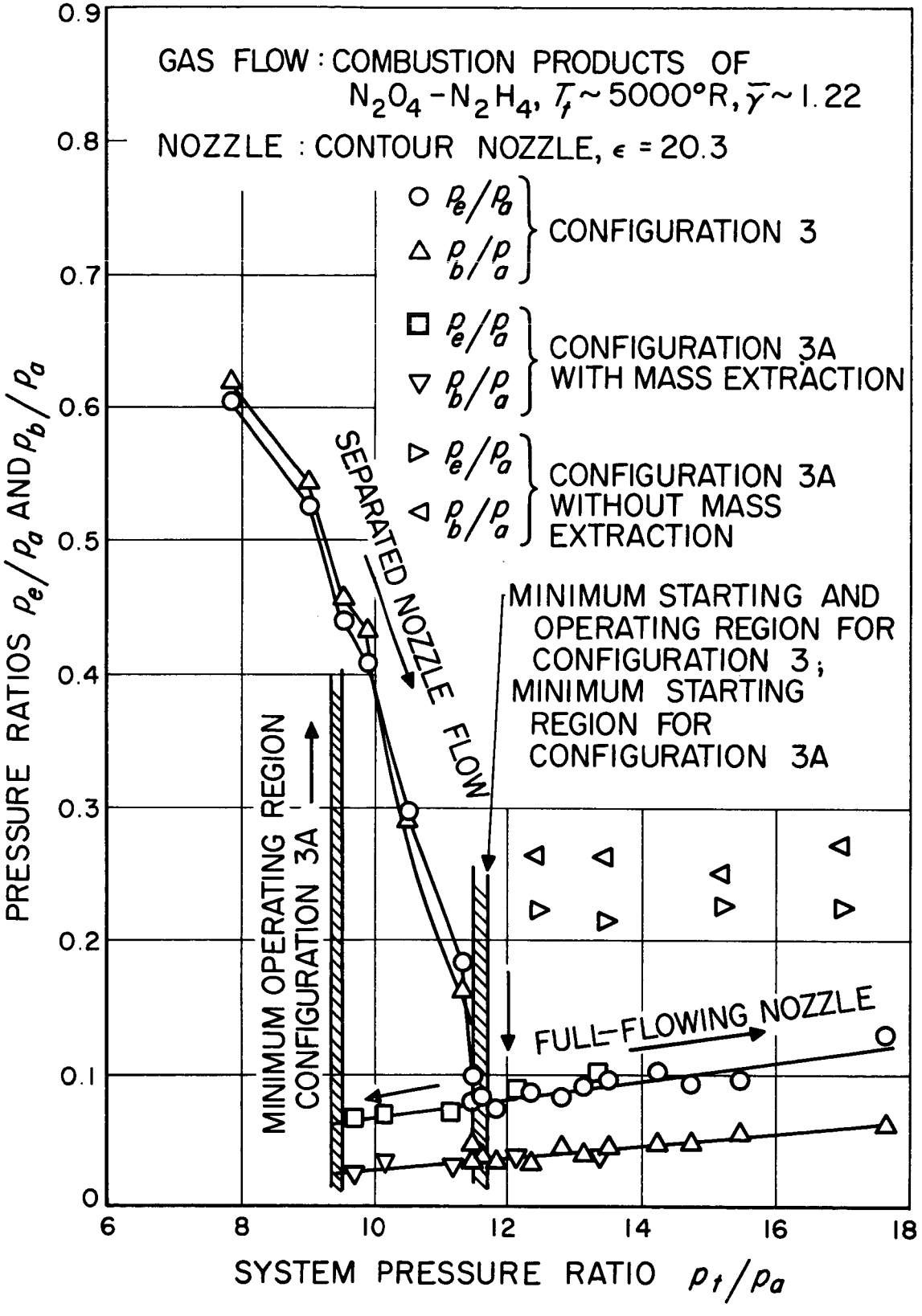

Fig. 13. Typical exhaust-diffuser performance, second-throat type diffuser, configuration 3, $\bar{\gamma} \sim 1.22$

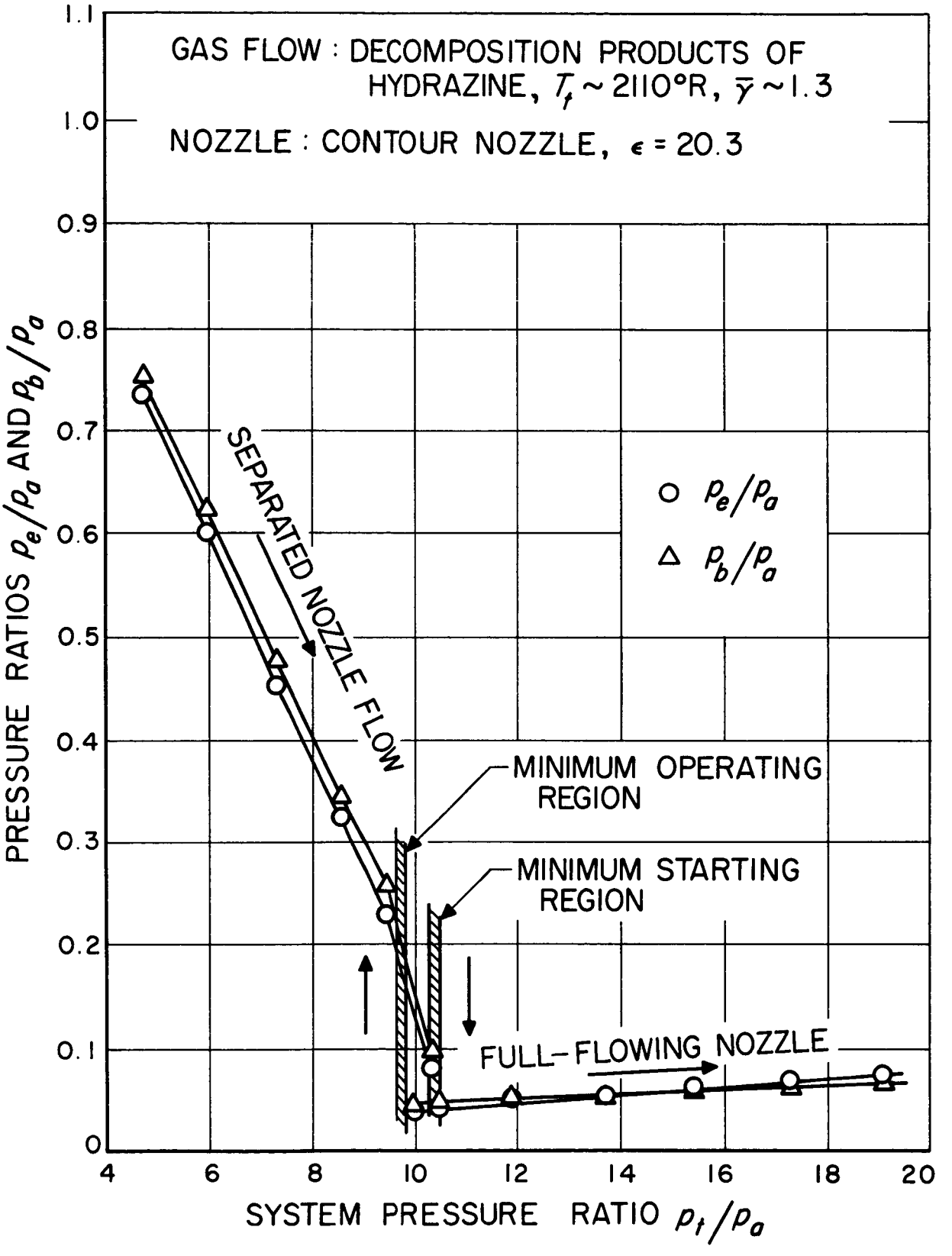

Fig. 14. Typical exhaust-diffuser performance, second-throat type diffuser, configuration 3, $\bar{\gamma} \sim 1.3$

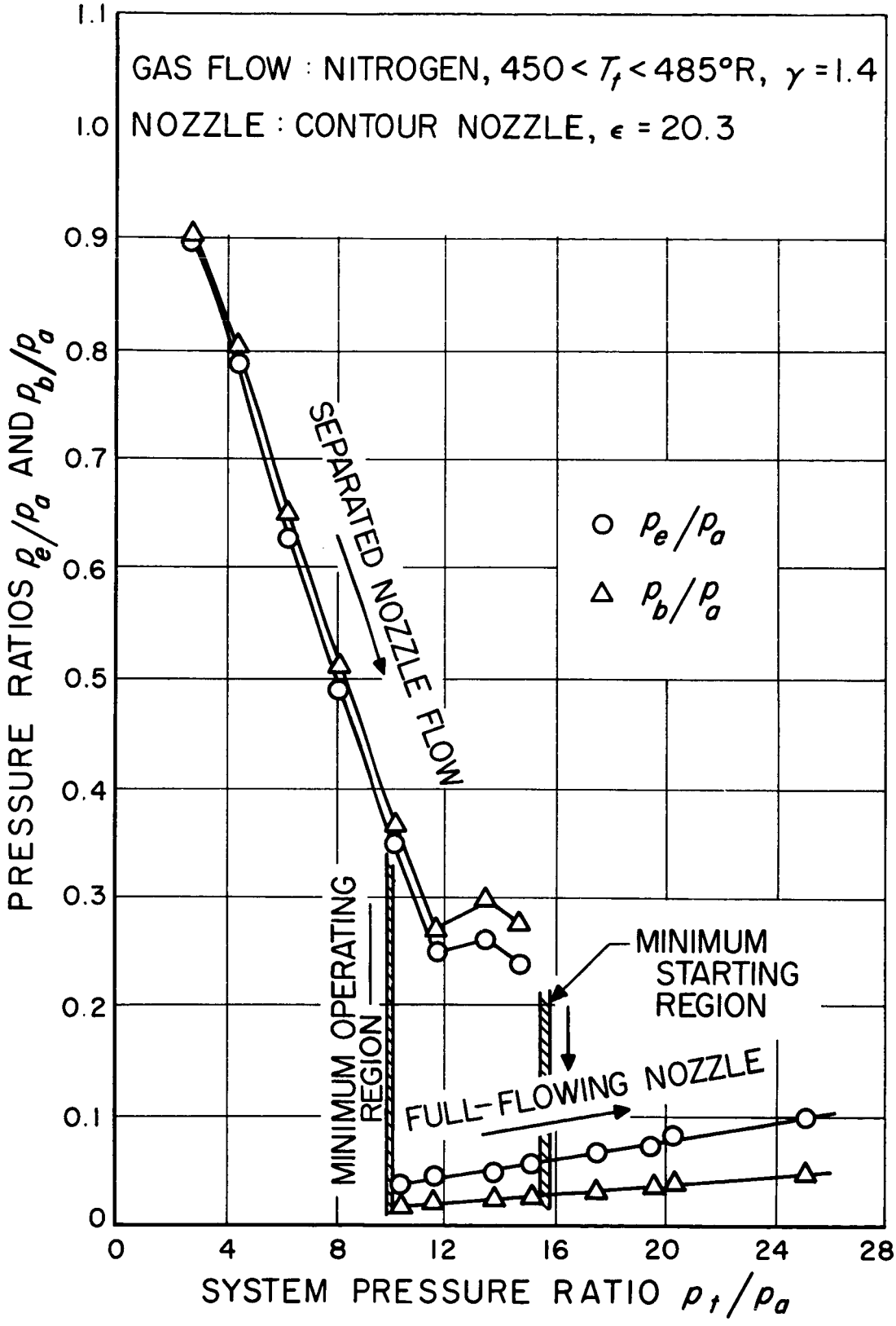

Fig. 15. Typical exhaust-diffuser performance, second-throat type diffuser, configuration 3, γ = 1.4

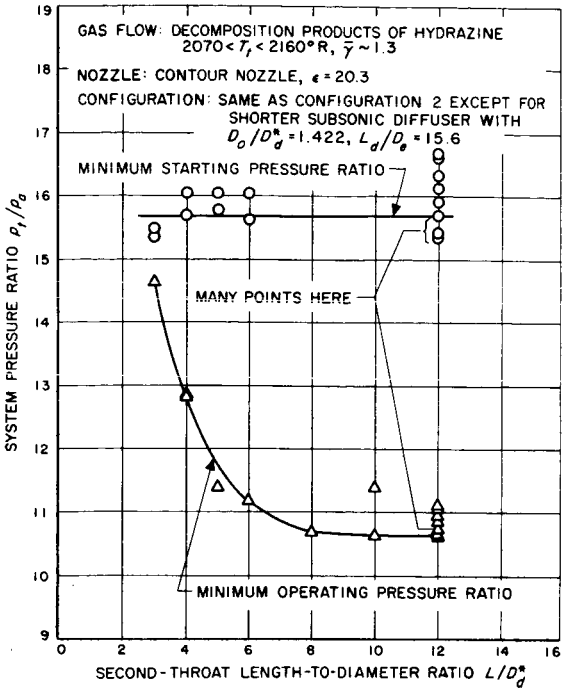

Fig. 16. Effect of second-throat length on the performance of configuration 2 with a fixed diffuser contraction ratio of 1.545

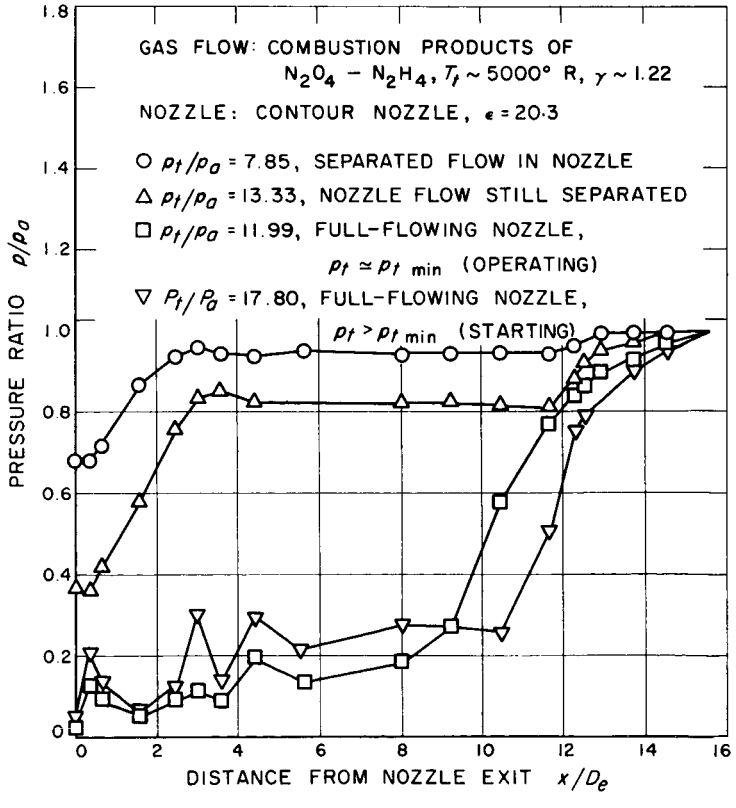

Fig. 17. Typical static-pressure distribution at the wall, second-throat type diffuser, configuration 2, $\bar{\gamma}$ ~ 1.22

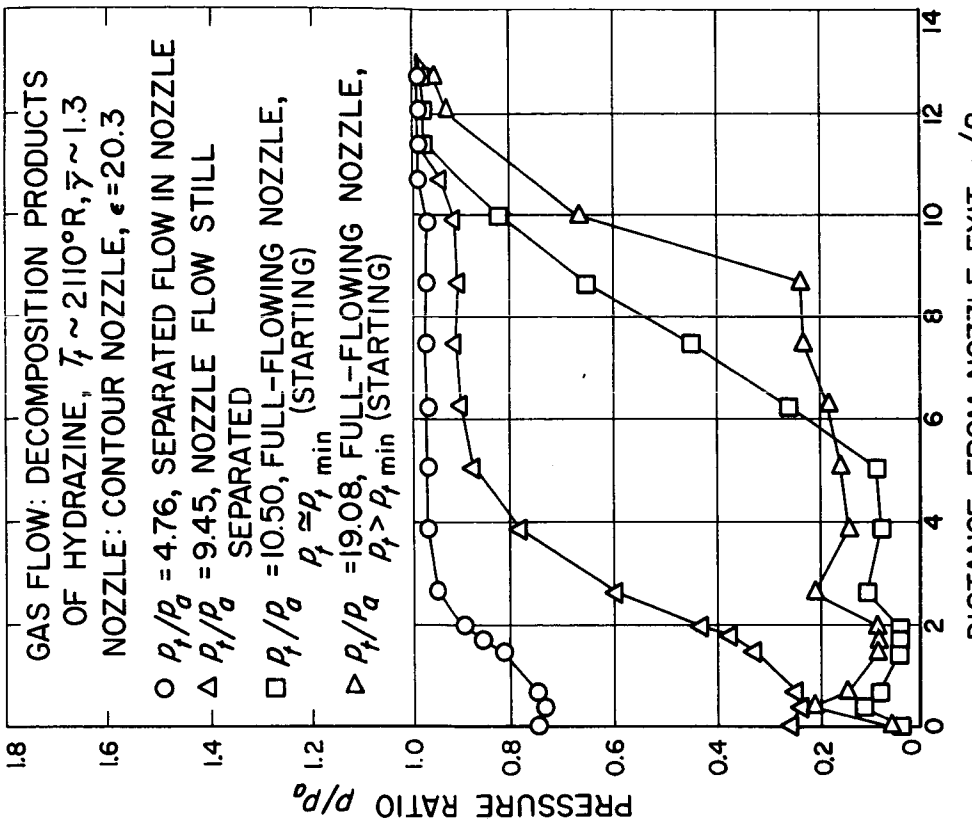

Fig. 19. Typical static-pressure distribution at the wall, second-throat type diffuser, configuration 3, $\gamma \sim 1.3$

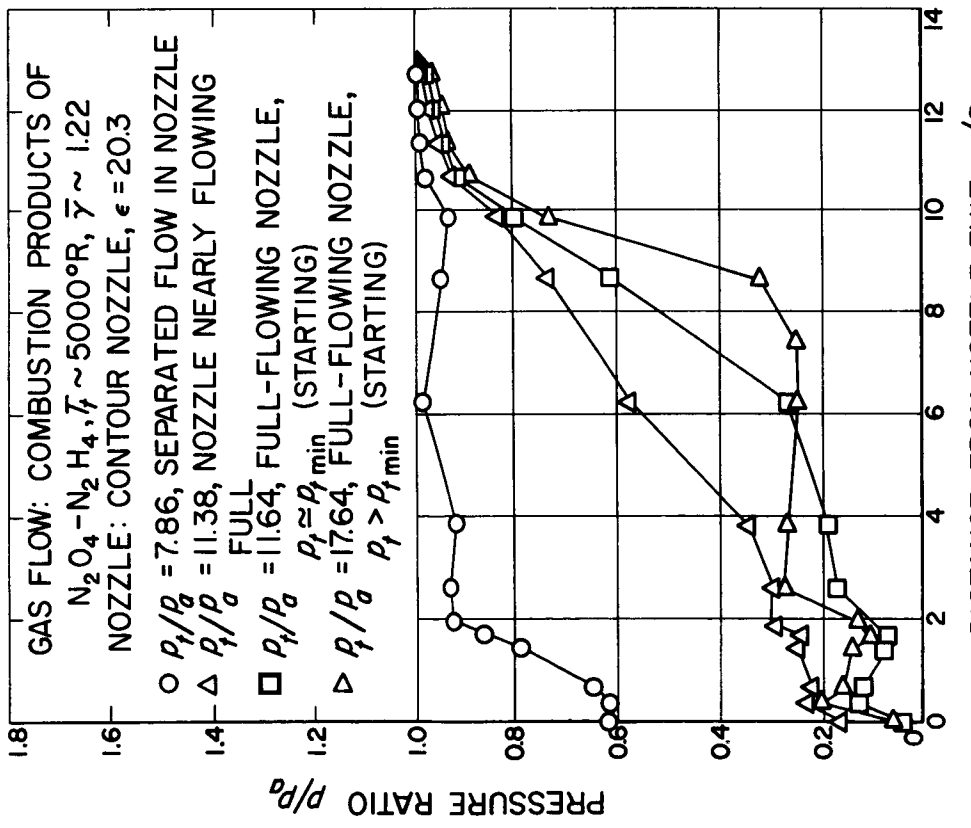

Fig. 18. Typical static-pressure distribution at the wall, second-throat type diffuser, configuration 3, $\gamma \sim 1.22$

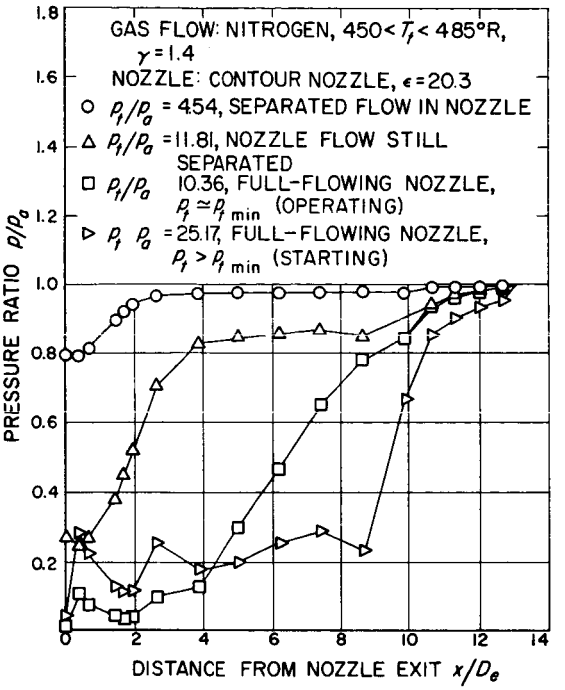

Fig. 20. Typical static-pressure distribution at the wall, second-throat type diffuser, configuration 3, γ = 1.4

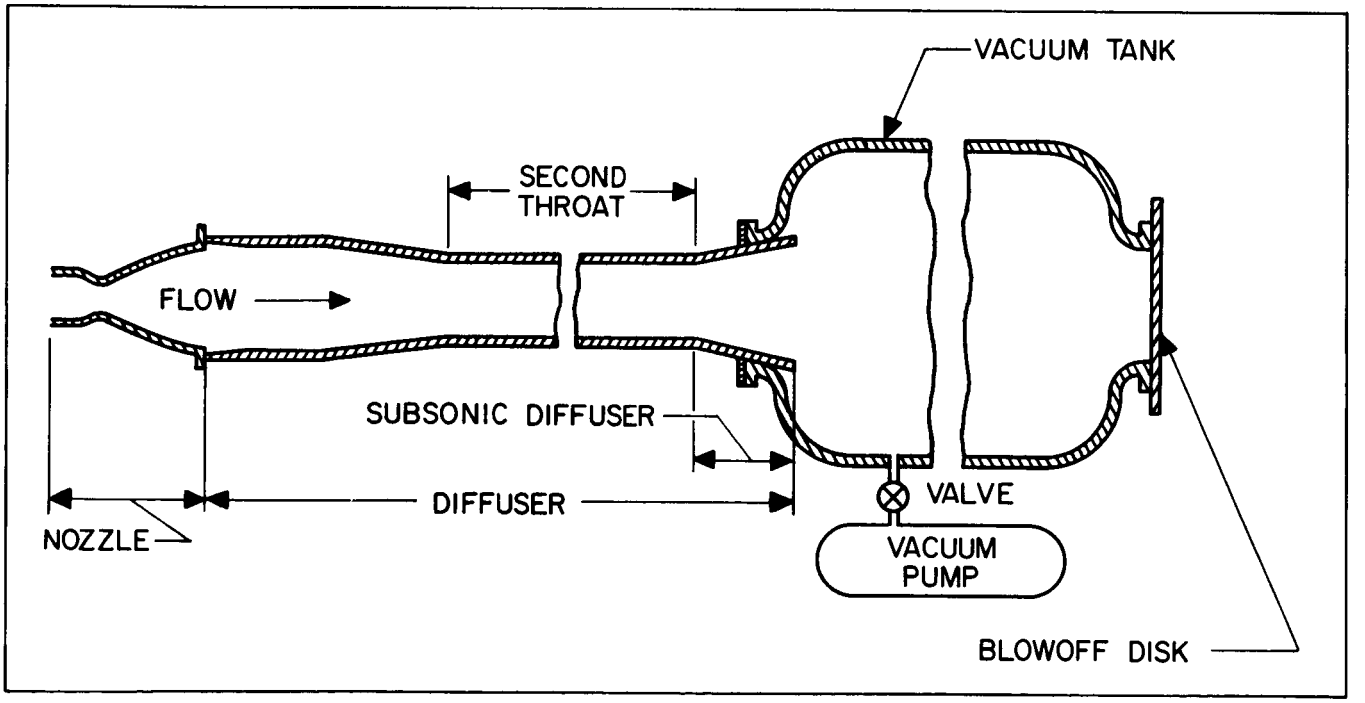

Fig. 21. Schematic arrangement of vacuum tank apparatus

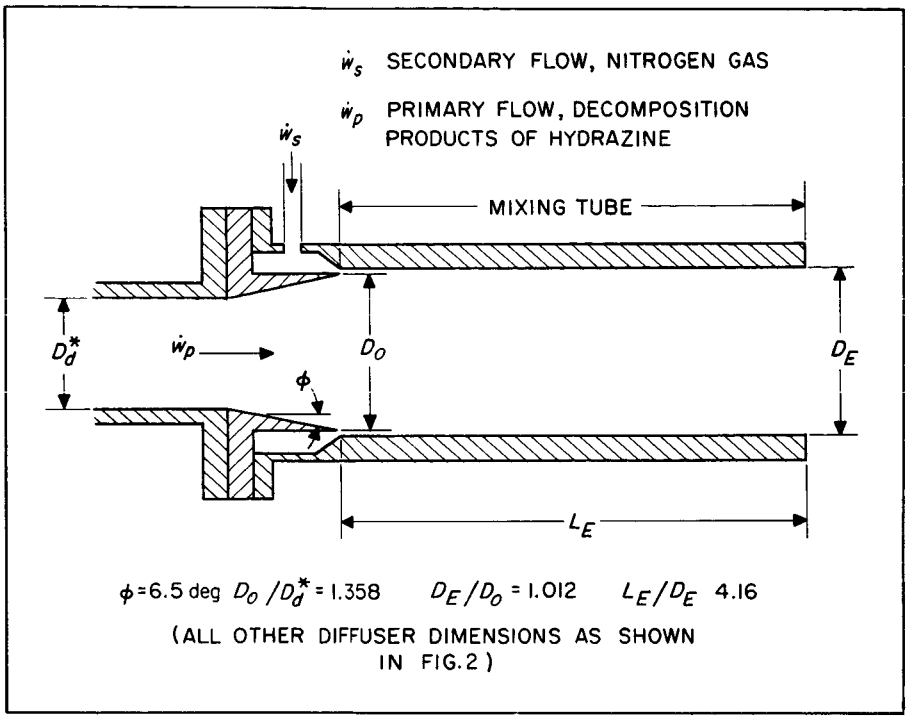

Fig. 22. Schematic arrangement of configuration 2 modified for annular ejection of a secondary gas at the exit of the subsonic diffuser

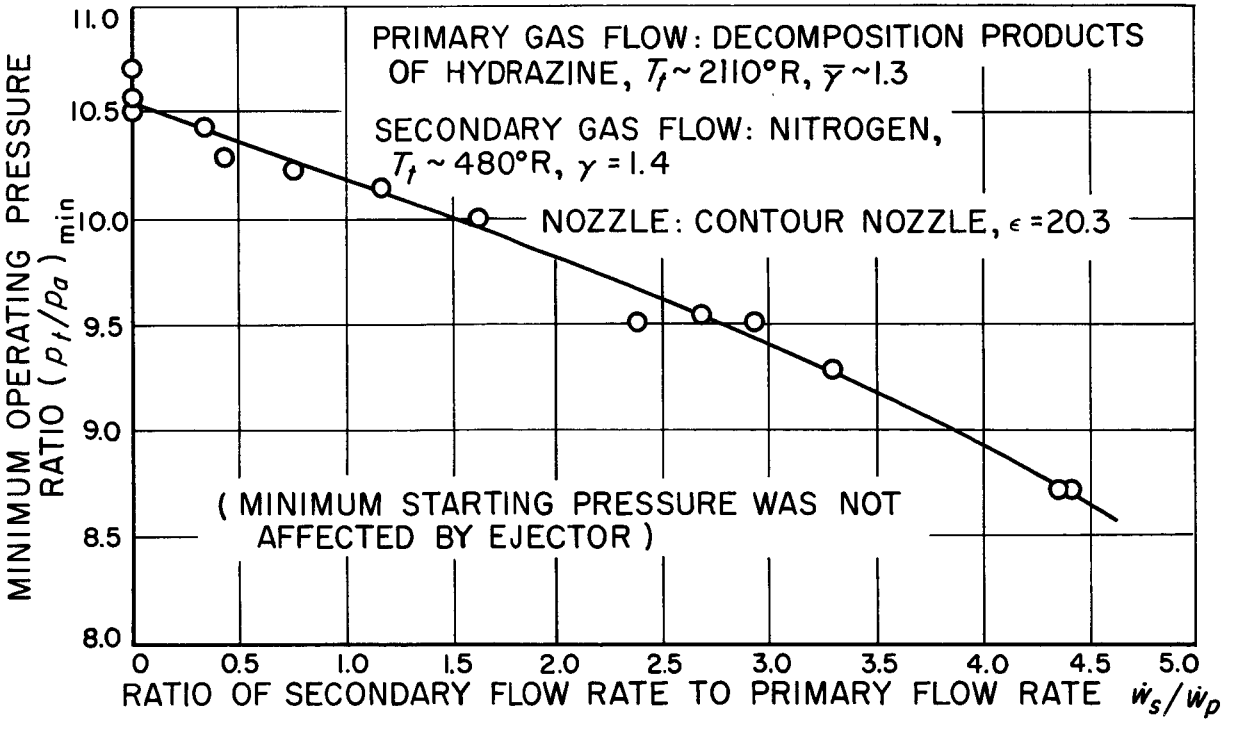

Fig. 23. Effect of nitrogen ejection at the diffuser exit on the operating performance of configuration 2

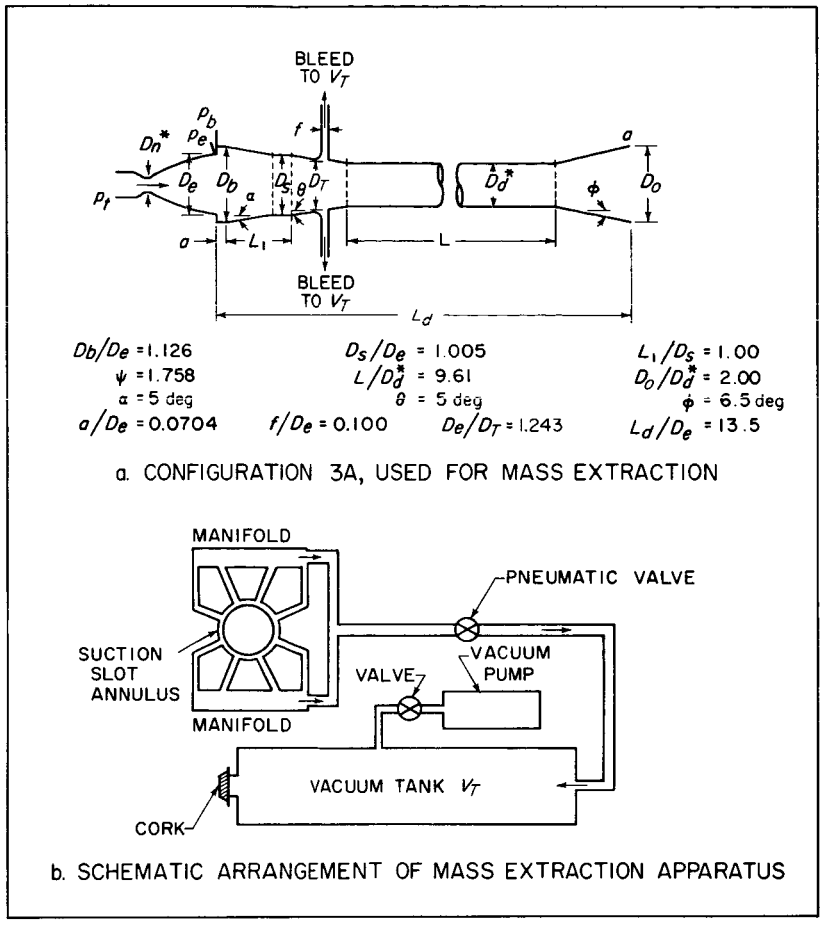

Fig. 24. Configuration and apparatus for primary-gas extraction on start

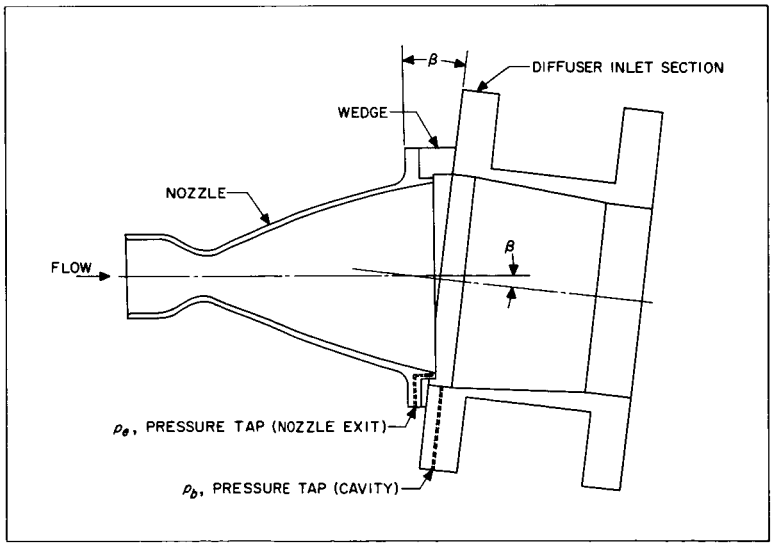

Fig. 25. Simulation of nozzle gimballing by insertion of a wedge between nozzle and diffuser inlet section

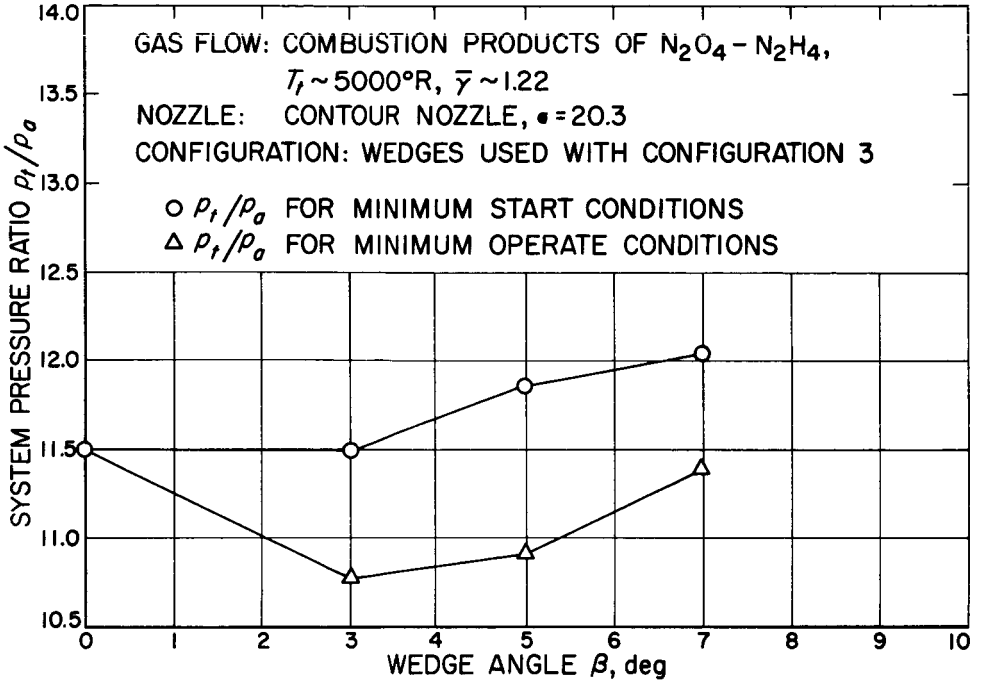

Fig. 26. Effect of angular misalignment between diffuser and nozzle axes on diffuser performance

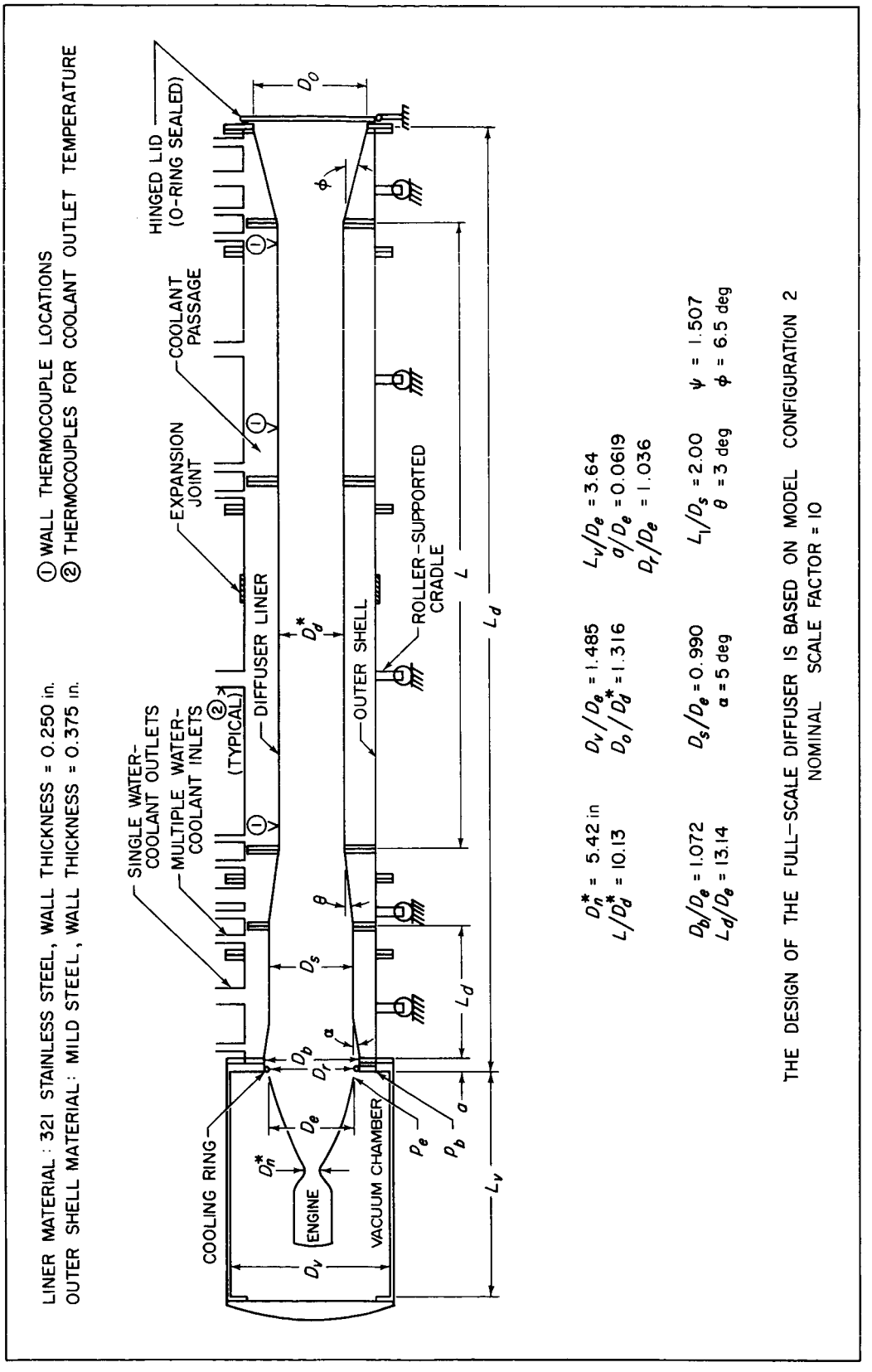

Fig. 27. An exhaust diffuser designed for use with a 6000-lb-thrust rocket engine having a nozzle-expansion-area ratio of 20.0

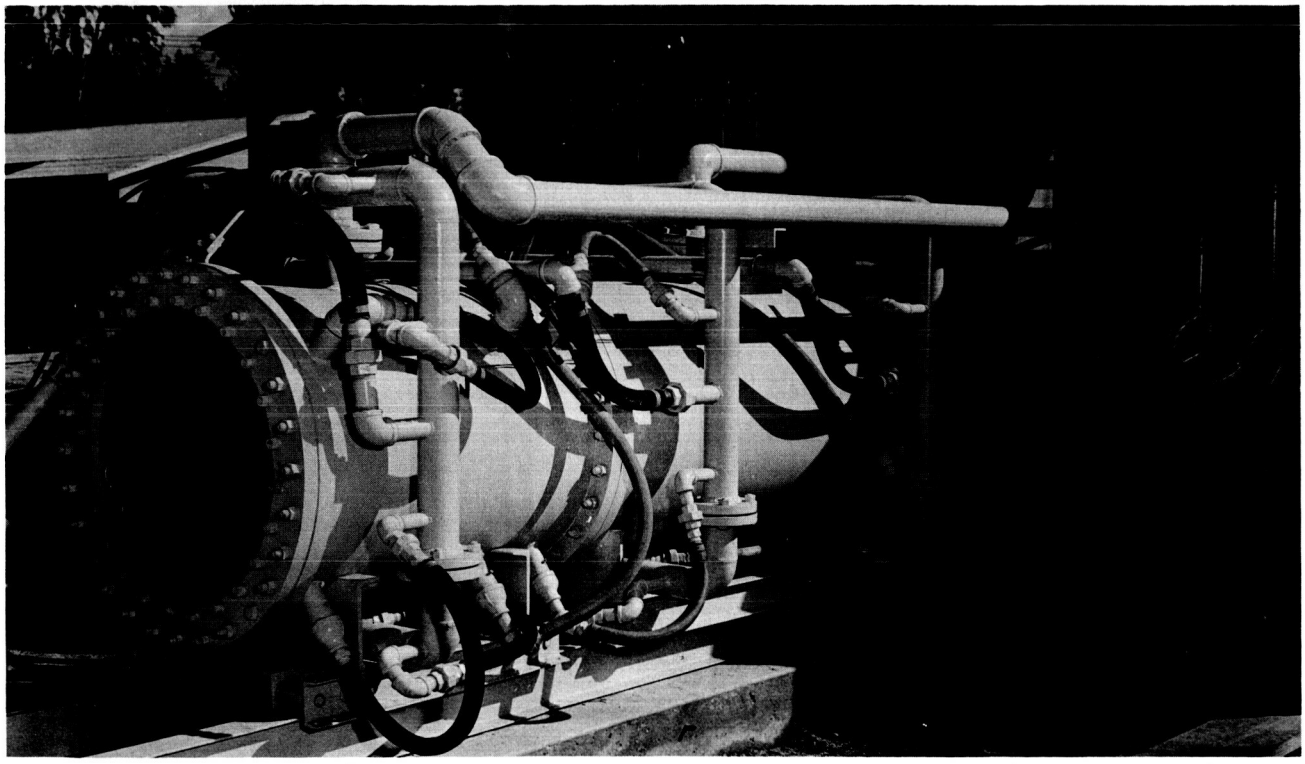

Fig. 28. View of exit end of full-scale exhaust diffuser

APPENDIX A. STARTING AND OPERATING AN EXHAUST DIFFUSER DOWNSTREAM OF A SUPERSONIC NOZZLE

It is assumed that shock-free, one-dimensional, isentropic flow occurs throughout the nozzle and the diffuser except at specified localities where a normal shock is assumed to exist. The configuration shown in Sketch A has been adopted for the purposes of this discussion. The total pressure at the nozzle inlet is denoted by p_t, the weight rate of flow by $\dot{w}$, and x and y denote gas properties upstream and downstream of a plane normal shock wave. It is further assumed that the static pressure downstream of a normal shock is the ambient or atmospheric pressure p_a.

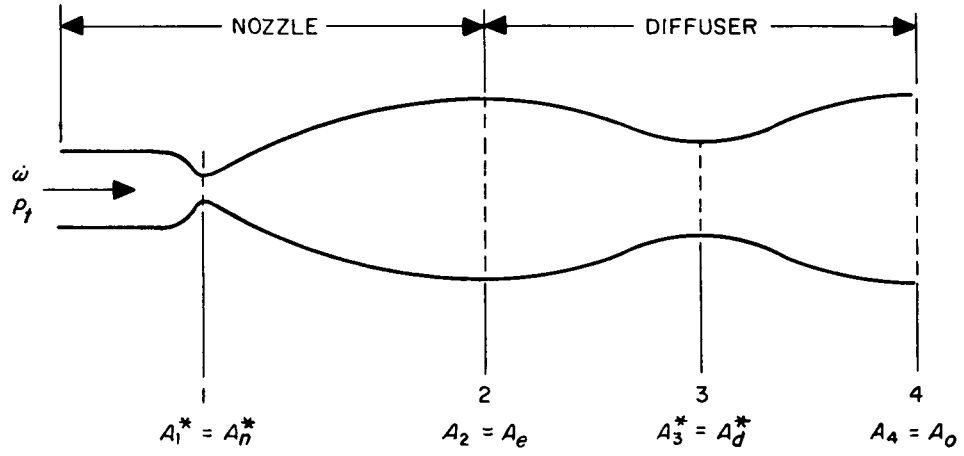

1. Starting Condition

One-dimensional-flow theory indicates that after the flow has been initiated through a supersonic nozzle and during the time interval that p_t is increasing, a normal shock forms in the divergent portion of the nozzle after sonic flow has been attained in the throat. For simplicity it is assumed in this

discussion that no diffuser exists. As p_t increases, the normal shock moves downstream until it is located at the nozzle exit diameter. The static pressure just upstream of the normal shock would then be the same as the nozzle exit pressure for an actual full-flowing nozzle, providing the value of p_t is the same and frictional effects are neglected. The static pressure downstream of the normal shock must be atmospheric since the flow there is subsonic; consequently, it is reasonable to compare the value of p_t for this condition with the starting chamber pressure obtained when the normal shock is replaced by an exhaust diffuser. The diffuser starting condition may then be expressed as:

$$\frac{p_t}{p_a} = \frac{p_t}{p_{2x}} \quad \frac{p_{2x}}{p_{2y}} = \frac{p_t}{p_{2x}} \quad \frac{p_{2x}}{p_a} \qquad [A-1]$$

where $p_{2x} = p_e$ and p_{2x}/p_{2y} is the static pressure ratio across a normal shock at location 2, assuming no diffuser exists. Curves based on Equation [A-1] are shown in Fig. 3.

2. Maximum Diffuser Contraction Ratio for Starting

It is assumed now that the diffuser is attached to the nozzle exit. The maximum weight rate of flow through a nozzle in which sonic velocity occurs at the throat is given by

$$\dot{w} = \frac{KA_1^* p_t}{\sqrt{T_t}}$$

where K is a coefficient depending on γ and R. By continuity, assuming that γ and R are not dependent on pressure or temperature, it will be seen that the product

of cross-sectional area and total pressure is constant throughout the nozzle-diffuser flow system. Based on one-dimensional-flow theory, a normal shock would progress along the divergent portion of the nozzle during the time interval when p_t is increasing, even with the diffuser attached. After the normal shock reaches the maximum diameter, it is swallowed and reappears at a slightly larger diameter in the exit cone or beyond the exit of the diffuser. The normal shock cannot be swallowed by the diffuser, however, unless A_3^* is large enough to allow all the weight flow rate to pass through the second throat when the normal shock is located at the maximum diameter upstream of this throat. Consequently, $p_{2ty} = p_{3t}$ is the total pressure downstream of this normal shock, assuming no losses between the shock and the diffuser throat. Therefore,

$$A_1^* p_t = A_3^* p_{2ty} \qquad [A-2]$$

From Equation [A-2],

$$\frac{A_2}{A_3^*} = \frac{A_2}{A_1^*} \frac{A_1^*}{A_3^*} = \frac{A_2}{A_1^*} \frac{p_{2ty}}{p_t}$$

or,

$$\frac{A_2}{A_3^*} = \psi_{max} = \epsilon \left(\frac{p_{2ty}}{p_t} \right) \qquad [A-3]$$

where p_{2ty}/p_t represents the total-to-total pressure ratio across a normal shock located at the nozzle exit, and ϵ is the nozzle-expansion-area ratio.

Equation [A-3] represents an expression for the maximum allowable diffuser contraction ratio for starting the diffuser. Curves based on Equation [A-3] are shown in Fig. 3.

3. Optimum Operating Condition

Consider that the configuration shown in Sketch A has been started in such a way that in the ideal case shock-free supersonic flow exists throughout the nozzle and the diffuser, and a normal shock wave is located at the diffuser exit. The nozzle inlet total pressure p_t is then reduced, causing the normal shock to move upstream until it becomes located at station 3, the minimum area of the diffuser A_d^*. Ideally, the value of p_t corresponding to this position of the shock would represent the minimum or optimum operating point of the nozzle-diffuser system, because any reduction in p_t would tend to displace the shock to a smaller area slightly upstream of the second throat and would result in shock return to the nozzle. An equation describing the minimum operating system pressure ratio can then be written as follows:

$$\frac{p_t}{p_a} = \frac{p_t}{p_{3x}} \quad \frac{p_{3x}}{p_{3y}} = \frac{p_t}{p_{3x}} \quad \frac{p_{3x}}{p_a} \qquad [A-4]$$

where p_t/p_{3x} is the isentropic flow condition corresponding to $A_3^*/A_1^* = A_d^*/A_n^*$ and p_{3x}/p_{3y} is the static-pressure ratio across a normal shock at station 3. Equation [A-4] is analogous to Equation [A-1] . Curves based on Equation [A-4] are shown in Fig. 3.

APPENDIX B. METHODS OF CALCULATING DIFFUSER EFFICIENCY

The enthalpy-entropy plot for the compression process occurring in the diffuser of Sketch A is shown in Sketch B.

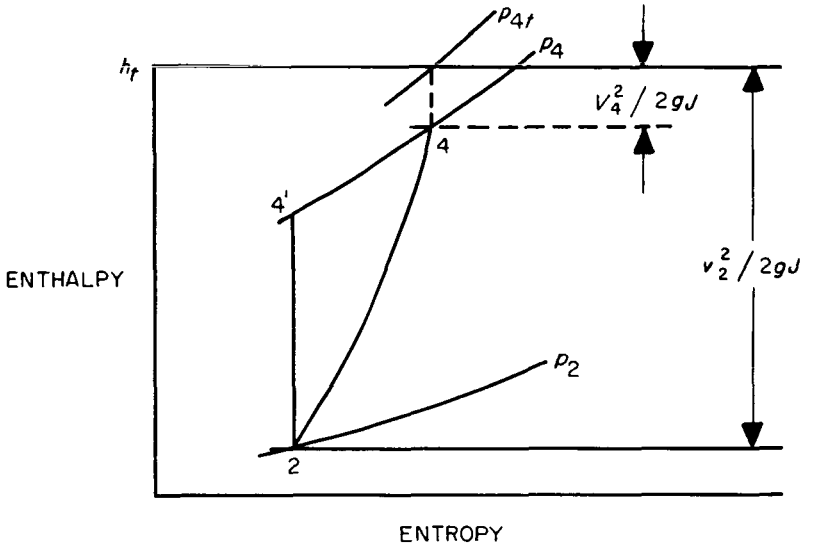

The vertical path between 2 and 4' represents the static enthalpy change for an isentropic compression between the static pressures p_2 and p_4. The path between 2 and 4 represents the static enthalpy change for the actual compression process between the same two pressure levels. The diffuser efficiency η_d is defined as the ratio of static enthalpy differences as follows:

$$\eta_d = \frac{h_4' - h_2}{h_4 - h_2} \simeq \frac{T_4' - T_2}{T_4 - T_2} \qquad [B\text{-}1]$$

Equation [B-1] can be put into the following form:

$$\eta_d = \frac{\left(\frac{p_4}{p_2}\right)^{\frac{\gamma - 1}{\gamma}} - 1}{\left(\frac{T_4}{T_2}\right) - 1} \qquad [B\text{-}2]$$

1. The Efficiency of a Normal Shock Located at the Nozzle Exit

The efficiency of a normal shock located at the nozzle exit, denoted by η_s, can be found by an appropriate application of Equation [B-2] as

$$\eta_s = \frac{\left(\frac{p_{2y}}{p_{2x}}\right)^{\frac{\gamma - 1}{\gamma}} - 1}{\left(\frac{T_{2y}}{T_{2x}}\right) - 1} \qquad [B\text{-}3]$$

where x and y again denote locations immediately upstream and downstream of a normal shock respectively. Curves based on Equation [B-3] are shown in Fig. 4.

An equation for the efficiency of a normal shock located at station 3 can be written. This equation is analogous to Equation [B-3]; however, such an equation would yield numerical values of efficiency only 2 to 3 per cent higher than obtained from Equation [B-3] for the same values of ϵ and γ.

2. Calculation of Diffuser Efficiency Using Experimental Data

Equation [B-2] is not in a form suitable for direct calculations of diffuser efficiency. In order to utilize the inlet total pressure to the nozzle, it is necessary to assume that isentropic flow conditions exist in the nozzle. Then p_t is used as the inlet total pressure to the diffuser. It is also necessary to

estimate the static temperature at the diffuser inlet and at the diffuser exit. The temperature $T_2 = T_b$ is found by assuming isentropic expansion from A_n^* to A_b. For convenience it is assumed that $T_o = T_t$, which is equivalent to assuming that the gas velocity at the diffuser exit is zero. The validity of the last assumption will be discussed later. Applying the assumptions just listed, Equation [B-2] can be written as

$$\eta_d = \frac{\left(\frac{p_a}{p_b}\right)^{\frac{\gamma - 1}{\gamma}} - 1}{\left(\frac{T_t}{T_b}\right) - 1} \qquad [B-4]$$

where $p_o = p_a$ = atmospheric pressure. Equation [B-4] can be further reduced to

$$\eta_d = \frac{\left(\frac{p_a}{p_b}\right)^{\frac{\gamma - 1}{\gamma}} - 1}{\left(\frac{p_t}{p_b}\right)^{\frac{\gamma - 1}{\gamma}} - 1} \qquad [B-5]$$

where both p_t and p_b are determined from experimental measurements. Equation [B-5] was used to calculate the diffuser efficiency as listed in Tables 2 and 3 with corresponding values plotted in Fig. 8. The primary objection to Equation [B-5] is that it involves the assumption of isentropic flow in the nozzle and also isentropic expansion from A_e to A_b. Experimentally, it was found that

the relationship between p_e and p_b did not appear to be consistent when comparing different configurations.

Using the gas properties listed in Table 1 and experimentally determined values of the weight rate of flow $\dot{w}$, estimates were made of the flow conditions at the diffuser exit. By utilizing the continuity equation $\dot{w} = \rho v A$, the definition of Mach number, and the perfect-gas law, the following equation can be written for the Mach number at the diffuser exit:

$$M_o = \frac{\dot{w}}{p_a A_o} \sqrt{\frac{RT_t}{g\gamma}} \qquad [B\text{-}6]$$

where it has been assumed that $T_o = T_t$ and $p_o = p_a$ at the diffuser exit. Also

$$\frac{T_t}{T_o} = \left[1 + \left(\frac{\gamma - 1}{2}\right) M_o^2\right] \qquad [B\text{-}7]$$

and

$$\frac{p_{t,o}}{p_a} = \left[1 + \left(\frac{\gamma - 1}{2}\right) M_o^2\right]^{\frac{\gamma}{\gamma - 1}} \qquad [B\text{-}8]$$

where $p_{t,o}$ denotes the total pressure at the diffuser exit. Calculations based on Equations [B-6], [B-7], and [B-8] are listed in Table B-1 for various experimental configurations. With the possible exception of configuration 1, the assumption $T_o = T_t$ appears to be quite valid since the Mach numbers at the diffuser exit are quite low.

Table B-1. Estimated flow properties at the diffuser exit, one-dimensional calculations based on the measured weight rate of flow

Model diffuser configuration	$\overline{\gamma}$	Minimum starting conditions			Minimum operating conditions		
		M_o	T_t/T_o	$p_{t,o}/p_a$ [1]	M_o	T_t/T_o	$p_{t,o}/p_a$ [1]
1 [2]	1.3	0.448	1.030	1.137	0.448	1.030	1.137
2	1.3	0.342	1.018	1.078	0.240	1.009	1.038
2	1.22	0.168	1.003	1.017	0.135	1.002	1.011
3	1.22	0.130	1.002	1.011	0.130	1.002	1.011
3	1.3	0.118	1.002	1.010	0.112	1.001	1.008
3	1.4	0.181	1.007	1.023	0.115	1.003	1.010
3A	1.22	0.130	1.002	1.011	0.113	1.001	1.008

[1] $p_{t,o}$ is the total pressure at the diffuser exit

[2] With $D_o/D_d^* = 1.422$

REFERENCES

1. Shapiro, A. H., The Dynamics and Thermodynamics of Compressible Fluid Flow, Vol. I, The Ronald Press Co., New York, 1953.

2. Neumann, E. P and Lusterwerk, F., "Supersonic Diffusers for Wind Tunnels", J. Appl. Mech., Trans. ASME, vol. 71, June, 1949, pp. 195-202.

3. Neumann, E. P., and Lusterwerk, F., "High-Efficiency Supersonic Diffusers", J. Aeron. Sci., vol. 18, June, 1951, pp. 369-374.

4. Lukasiewicz, J., "Diffusers for Supersonic Wind Tunnels", J. Aeron. Sci., vol. 20, Sept., 1953, pp. 617-626.

5. Fortini, A., Performance Investigation of a Nonpumping Rocket-Ejector System for Altitude Simulation, NASA Tech. Note D-257, December, 1959.

6. Jones, W. L., Price, H. G. Jr., and Lorenzo, C. F., Experimental Study of Zero-Flow Ejectors Using Gaseous Nitrogen, NASA Tech. Note D-203, March, 1960.

7. Emmons, H. W., Fundamentals of Gas Dynamics, Vol. III of High Speed Aerodynamics and Jet Propulsion Series, Princeton University Press, Princeton, New Jersey, 1958.

8. Patterson, A. M., "Improvement of Pressure Recovery of a Fixed Diffuser by Means of Suction", J. Aeron. Sci., vol. 20, June, 1953, pp. 430-432.

9. Patterson, A. M., Factors Affecting the Performance of Supersonic Diffusers, Univ. Toronto, Inst. of Aerophysics, UTIA Report No. 23, Dec., 1952.

BIBLIOGRAPHY

Barton, D. L., and Taylor, D., An Investigation of Ejectors Without Induced Flow-Phase 1, AEDC Tech. Note 59-145, December, 1959.

DeLeo, R. V., An Experimental Investigation of the Use of Hot Gas Ejectors for Boundary Layer Control - Part III, WADC Tech. Report 52-128, June, 1958.

Fabri, J., and Paulon, J., Theory and Experiments on Supersonic Air-to-Air Ejectors, NACA Tech. Memo 1410, September, 1958.

Fortini, A., Hendrix, C. D., and Huff, V. N., Experimental Altitude Performance of JP-4 Fuel and Liquid Oxygen Rocket Engine with an Area Ratio of 48, NASA Memo 5-14-59E, May, 1959.

Hasel, L. E., and Sinclair, A. R., A Preliminary Investigation of Methods for Improving the Pressure-Recovery Characteristics of Variable-Geometry Supersonic-Subsonic Diffuser Systems, NACA Research Memo L57H02, Oct., 1957.

Hensel, R. W., and Matt, H. K., Full Scale Propulsion Testing in Wind Tunnels, AEDC TR 59-9, May, 1959.

Hermann, R., and Thompson, K. O., Application of the Generalized Free Jet Analysis to Conventional Variable Geometry Free Jet Tunnel, AEDC Tech Note 59-72, July, 1959.

Kantrowitz, A., Discussion of reference (1), "Supersonic Diffusers for Wind Tunnels", by E. P. Neumann and F. Lusterwerk, J. Appl. Mech., Trans. ASME, Vol. 71, pp. 417-418, Dec., 1949.

Kline, S. J., Abbot, D. E., and Fox, R. W., Optimum Design of Straight-Wall Diffusers, ASME Paper No. 58-A-137, Presented at Annual Meeting, Nov.-Dec., 1958.

Kyser, J. B., Design and Performance of a Variable Geometry Diffuser for an Axisymmetric Wind Tunnel, Defense Research Laboratory, University of Texas, Austin, DRL-370, Feb., 1956.

Lightner, I. C., Altitude Facility Rocket Testing, ARS Paper No. 996-59, Presented at 14th Annual ARS Meeting, Washington, D. C., Nov., 1959.

Pierpont, P. K., Investigation of Suction-Slot Shapes for Controlling a Turbulent Boundary Layer, NACA Tech. Note 1292, June, 1947.

Rhodes, R. P., Evaluation of Hot-Water-Driven Diffuser Ejectors, AEDC Tech Note 59-127, Nov., 1959.